1   **Iron Isotope Systematics in Estuaries: The case of North River,**

2   **Massachusetts (USA)**

3

4   Raphaelle Escoube[1,2], Olivier J. Rouxel[1*], Edward Sholkovitz[1] and Olivier

5   F.X. Donard[2]

6

7   1.   Marine Chemistry & Geochemistry Dept., Woods Hole Oceanographic

8   Institution, Woods Hole, MA02543, USA

9   2.   LCABIE, U. Pau et Pays de l'Adour, CNRS UMR 525, Hélioparc

10   64053 Pau, France

11

12   *Corresponding author: orouxel@whoi.edu*

13

14

15   *Geochimica et Cosmochimica Acta*

16

17

18

Abstract:

19

20   Recent studies have suggested that rivers may present an isotopically light Fe

21   source to the oceans. Since the input of dissolved iron from river water is generally

22   controlled by flocculation processes that occur during estuarine mixing, it is important to

23   investigate potential fractionation of Fe-isotopes during this process. In this study, we

24   investigate the influence of the flocculation of Fe-rich colloids on the iron isotope

25   composition of pristine estuarine waters and suspended particles. The samples were

26   collected along a salinity gradient from the fresh water to the ocean in the North River

27   estuary (MA, USA). Estuarine samples were filtered at 0.22 µm and the iron isotope

28   composition of the two fractions (dissolved and particles) were analyzed using high-

29   resolution MC-ICP-MS after chemical purification. Dissolved iron results show positive

30   δ^{56}Fe values (with an average of 0.43 ± 0.04 ‰) relative to the IRMM-14 standard and do

31   not display any relationships with salinity or with percentage of colloid flocculation. The

32   iron isotopic composition of the particles suspended in fresh water is characterized by

33   more negative δ^{56}Fe values than for dissolved Fe and correlate with the percentage of Fe

34   flocculation. Particulate δ^{56}Fe values vary from -0.09‰ at no flocculation to ~ 0.1‰ at

35   the flocculation maximum, which reflect mixing effects between river-borne particles,

36   lithogenic particles derived from coastal seawaters and newly precipitated colloids. Since

37   the process of flocculation produces minimal Fe-isotope fractionation in the dissolved Fe

38   pool, we suggest that the pristine iron isotope composition of fresh water is preserved

39   during estuarine mixing and that the value of the global riverine source into the ocean can

40   be identified from the fresh water values. However, this study also suggests that δ^{56}Fe

41   composition of rivers can also be characterized by more positive δ^{56}Fe values (up to 0.3

42   per mil) relative to the crust than previously reported. In order to improve our current

43   understanding of the oceanic iron isotope cycling, further work is now required to

44   determine the processes controlling the fractionation of Fe isotopes during continental

45   run-off.

46

47

48   ***Keywords:*** *iron isotopes, rivers, estuary, flocculation, iron cycle, colloids*

49

50

51

1. Introduction

52

53

54   Although iron (Fe) is the 4th most abundant element in the Earth's crust (Taylor et al.,

55   1983; Wedepohl, 1995), its concentration decreases to trace levels (< 1 nM) in the ocean

56   (Wu et al., 2001; Boyle et al., 2005; Johnson et al., 1997). Because Fe acts as an essential

57   micronutrient in biological processes (e.g. phytoplankton growth), iron concentration in

58   the ocean is considered to be a limiting factor for primary productivity in large regions of

59   the open ocean (Martin, 1990; Lefevre and Watson, 1999; Archer and Johnson, 2000;

60   Boyd et al., 2000; Christian et al., 2002; Moore et al., 2002; Moore et al., 2004). The main

61   sources of dissolved Fe into the ocean are wet and dry deposition from the atmosphere,

62   input from rivers, re-suspended sediment, pore water from continental shelves and

63   hydrothermal vents (e.g. Wells et al., 1995; Elderfield and Schultz, 1996; Johnson et al.,

64   1999; Elrod et al., 2004; Jickells et al., 2005; Bennett et al., 2008).

65   Iron isotopes exhibit natural δ^{56}Fe variations of ~5‰ (Anbar, 2003; Beard and

66   Johnson, 2004; Dauphas and Rouxel, 2006; Johnson and Beard, 2006) and provide

67   potential new approaches to constrain the relative contribution of Fe sources in the

68   oceans, and to improve our understanding of how Fe is mobilized from source regions

69   (i.e. rivers, sediments) and transported into the ocean. In practice, the Fe isotopic

70   composition of the various sources to the oceans is not well documented but recent

71   studies have suggested that major sources of iron provide significant inputs of low- δ^{56}Fe

72   iron to the oceans. In fact, continental run-off (Fantle and De Paolo, 2004; Bergquist and

73   Boyle, 2006), hydrothermal sources (Beard et al., 2003a; Rouxel et al., 2008a), diagenetic

74   pore fluids from shelf sediments and subterranean estuaries (Severmann et al., 2006;

75   Rouxel et al., 2008b) have been suggested as potential negative δ^{56}Fe sources in seawater.

76   The focus of this paper will be on the river and estuarine component of the iron

77   geochemical cycle. We present a comprehensive study of the variation in Fe isotope

78   composition of dissolved and particulate iron across the river/ocean mixing zone.

79   Large scale removal of river-borne dissolved Fe is a common feature of estuaries.

80   Hence, the river input of dissolved Fe into the ocean is greatly modified by the salt-

81   induced flocculation of Fe-humic-colloids that occurs during the mixing of fresh water

82   and seawater (Eckert and Sholkovitz, 1976; Sholkovitz, 1976, 1978; Boyle et al., 1977;

83   Mayer, 1982; Hunter, 1990).

84   The estuarine reactivity of the river-borne colloids depends on the speciation of iron, a

85   factor which may also control Fe-isotope composition (e.g. Brantley et al., 2001; Brantley

86   et al., 2004; Johnson et al., 2004). In a preliminary study, Bergquist and Boyle (2006)

87   reported the Fe-isotope composition of colloids precipitated during river water–seawater

88   mixing experiments using the Solimões River water. Although the isotopic shifts in the

89   flocculent (+0.2‰) was small and close to the analytical uncertainty, those results imply

90   that the remaining Fe in solution may be isotopically lighter than the Fe in the river water

91   end-member. Hence, it is presently unknown whether flocculation processes in natural

92   estuarine systems can significantly affect the iron isotope composition of riverine

93   discharged Fe to seawater.

94   The first aim of this paper is to determine if the large scale removal of dissolved Fe

95   during estuarine mixing will affect the iron isotope values of estuarine waters. Since

96   estuaries act like a "filter" for terrestrially-derived dissolved iron, it is important to test

97   whether this "filter effect" modifies the isotopic value of river-borne Fe within the

98   estuaries mixing zone. Our second objective is to characterize the Fe-isotope systematics

99   between dissolved and particulate pools in estuaries and to assess the impact of rivers on

100   the Fe-isotope composition of seawater. To this end, a series of model equations will be

101   developed and applied to a set of dissolved and particulate samples from the North River

102   estuary.

103

2. Material and location

105   We collected water and suspended particles along the North River Estuary

106   (Massachusetts, USA) in October 2006 (**Fig.1**). This river was chosen because of its high

107   concentration of dissolved organic matter and colloidal iron, its proximity and convenient

108   access as well as its limited urbanization setting. The waters of the North River and its

109   estuary are distinctly yellow-brown in color due to dissolved humic substances. Typically,

110   this type of river contains dissolved Fe in the form of colloids (Sholkovitz, 1976; Ross

111   and Sherrell, 1999). The estuary watershed extends over 85 km^2 and is primarily

112   composed of salt marshes with Paleozoic and Precambrian igneous and metasedimentary

113   rocks. The estuary can be physically characterized as partially mixed to vertically

114   homogeneous. As such, the surface water salinity changes gradually along the narrow

115   channel of the estuary; this allowed us to collect samples with small (0.2 PSU) differences

116   in salinity (**Fig.1**).

117   A 13' fiberglass boat was used to collect water samples at high and low tide in

118   October 2006 (NR1, **Table 1**). Samples were collected in the central part of the river and

119   estuary by attaching acid-washed 1L polyethylene (LPDE) bottles to a 2 m long plastic

120   pole and dipping the bottle to a depth of 30 cm depth. Salinity and temperature were

121   measured on site using an onboard YSI® probe. Salinity data are presented in Table 1.

122   During the sampling time, water temperature was restricted between 13.5 and 12°C. One

123   month later, a second set of freshwater samples (NR2) was collected from the North River

124   in the town of Hanover, MA at the Elm St park at approximately 2 km up stream of the

125   NR1 sample. This upstream site never experiences the intrusion of salt water and then

126   represents fresh water background. The NR2 samples were collected to obtain more

127   isotopic data for the fresh water end-member; these samples were also used for more

128   complex types of filtration procedures.

129

130   Two samples of river water from the Connecticut River and Mullica River were also

131   analyzed for the Fe-isotope composition of their dissolved Fe pool. The Connecticut

132   River drains a large region of northeast North America and is the largest river entering the

133   ocean in New England (Garvine, 1975). Like the North River, the Mullica River (New

134   Jersey, USA) contains high concentrations of humic-type organic matter and colloidal Fe

135   (Yan et al., 1990; Ross and Sherrell, 1999). Humic substances impart a dark yellow-

136   brown color to the river water.

137

138   **3. Analytical method**

139

140   *3.1. Sample filtration*

141   We operationally define "dissolved iron" as the Fe that passed through a 0.22 μm

142   filter. This < 0.22 μm fraction contains colloidal and truly dissolved (i.e. soluble) Fe

143   pools. Although not measured, the soluble Fe pool is operationally defined as a non-

144   colloidal fraction that is not affected by flocculation process in the estuary and is likely

145   composed of organically bound iron. The particulate fraction consists of particles retained

146   by 0.22 μm filters; this > 0.22 μm fraction contains the suspended sediment as well as

147   newly precipitated colloids in the estuary. Less than 8 hours after sample collection, the

148   water samples from the North River estuary were pressure (using N_2 at 31 PSI) filtered

149   through Durapore^{TM} membrane type filters manufactured by Millipore Corp.. The filters

150   were 47 mm in diameter and had a nominal pore size of 0.22 μm. Polycarbonate plastic

151   filter holders by Sartorius Ltd. were acid cleaned and used for the pressure filtration step.

152   Filtered water samples were acidified to pH ~ 2 using ultra-pure (Optima-grade) 1N HCl.

153   For each sample, a non-acidified aliquot of 15 mL was kept for color measurement. The

154   filters were stored dried.

155

156   One of the river water samples, collected upstream of the estuary in November 2006

157   (sample NR2), was pressure filtered as describe above. A second sample was handled

158   differently; it was pumped through a Millipore Millipak[TM] cartridge filter unit that

159   contained 0.22 μm pore size Durapore[TM] filter material. The water obtained from the

160   pressure filtering method was then refiltered in parallel through 0.1, 0.05 and 0.025 μm

161   membrane filters. This filtration scheme was designed to characterize the colloids within

162   the dissolved pool (<0.22 μm) of Fe. The three fractions collected correspond to three

163   size ranges of colloids: 0.22-0.1 μm; 0.22-0.05 μm and 0.22-0.025 μm.

164   The Mullica River water was filtered using a hand-held all-plastic syringe with a 0.22

165   μm pore size filter unit from Millipore. The water was filtered on a small boat on June

166   26th 2007 and acidified on the spot. The Connecticut River water was collected off a

167   small boat, pressure filtered on May 22nd 2007 and acidified as described for the North

168   River.

169

170   *3.2. Chemical analysis*

171   According to Sholkovitz (1976), the adsorption measurement of the UV-Vis

172   spectra of unacidified filtered water samples at wavelengths of 350 nm and 465 nm

173   provide an approximation of the humic acid content of the filtered samples.   These

174   measurements were carried out in a 5 cm quartz cell. Total dissolved iron concentrations

175   of the acidified filtered water samples were measured by UV-Vis spectrophotometry

176   using the Ferrozine method modified from Stookey (1970). A reductant (Hydroxylamine

177   HCl) was used to obtain concentrations of total dissolved Fe. Measurements were

178   performed at a wavelength of 562 nm in 5 cm quartz cell.

179   Multi-elemental analysis of the acidified filtered water and digests of the

180   suspended particles were carried out on a ICP-MS (Finnigan Element 2). The filters were

181   leached overnight with 6 mL of 7N distilled HNO_3 in 15 mL closed Teflon vials on a hot

182   plate at 80°C. The solutions were then slowly evaporated to dryness. A second dissolution

183   step using 0.5 mL of concentrated ultrapure HF and 2 mL of concentrated distilled HCl

184   was then used to obtain a total digestion of the particles. 5 mL of distilled and

185   concentrated HNO_3 and 1 mL of H_2O_2 were added and the filters were removed before the

186   solution was taken to dryness. The solid residue was dissolved in 10mL of 2% HNO_3

187   (Optima grade) and an aliquot was further diluted for multi elemental ICP-MS analyses.

188   The remaining solution was saved for Fe-isotope analysis. Acidified water samples were

189   diluted to 1:7 with 2% HNO_3 (Optima grade). Indium solution was added to a final

190   concentration of 5 ppb to correct for ICP MS sensitivity changes due to matrix effects.

191   Four multi element standards with a salinity of 0, 0.9, 1.4, and 3.3 respectively were

192   analyzed as calibration points. Water analysis reported in **Table 1** includes Fe, Ca, Mo,

193   Mn, Al while Ti, Cr, Co, Zn and Cu were below detection limit and are not reported.

194   Particulate concentrations for Al, Fe, Ti, Ca and Mn are reported in Table 2.

195

196   *3.3. Iron isotope analysis*

197   A volume of not more than ~40 mL of estuarine water with a salinity < 15 was

198   evaporated to dryness in Teflon vials with 1 mL of concentrated distilled HNO_3 to release

199   the iron from organic complexes. The maximum operational volume for saline water

200   reflects the high load of salts that prevent evaporating larger volume of waters without

201   subsequent problems during chromatography separation. Consequently, Fe-isotope

202   analysis were performed only for samples with <15 salinity. The acid solution was taken

203   to dryness at 80°C on a hot plate. A subsequent evaporation was done with 10 mL of

204   distilled 7N HNO_3 with 1 mL of H_2O_2 (ultrapure grade). For the particulate analysis, the

205   solution obtained after complete digestion (section 3.1) was evaporated on a hot plate. For

206   both river water and particle samples, the solid residue were dissolved with 4 mL of

207   distilled 6N HCl and one drop of H_2O_2 to ensure the complete oxidation of Fe. This

208   solution was loaded onto a chromatography column filled with 1.5mL (wet volume) of

209   anion exchange resin (AG1-X8, Bio-rad) previously cleaned with 10 mL of 3N HNO_3 and

210   10 mL of 18mΩ H_2O. Prior to sample loading, the resin was conditioned with 5 mL of

211   distilled 2% HCl followed by 2.5 mL of distilled 6N HCl. After loading the sample, 25

212   mL of distilled 6N HCl was passed through the resin to elute the matrix. Iron is then

213   eluted with 12.5 mL of distilled 0.24N HCl and collected in 15 mL Teflon vials. Samples

214   were evaporated to dryness on a hot plate at 80°C and dissolved with 3mL of distilled

215   0.24N HNO_3 ready for isotope analysis.

216   Fe isotope compositions were determined with a Finnigan *Neptune* multicollector

217   inductively coupled plasma mass spectrometry (MC-ICPMS) at WHOI using the method

218   described in Rouxel et al. (2005; 2008a). The *Neptune* instrument permits high precision

219   measurement of Fe isotope ratios without argon interferences using the high-mass
220   resolution mode (Weyer and Schwieters, 2003; Poitrasson and Freydier, 2005). Mass
221   resolution power of about 8000 (medium resolution mode) was used to resolve isobaric
222   interferences, such as ArO on ^{56}Fe, ArOH on ^{57}Fe, and ArN on ^{54}Fe. Instrumental mass
223   bias is corrected using Ni isotopes as internal standards. The method, which has proved to
224   be reliable for the Neptune instrument, involves deriving the instrumental mass bias by
225   simultaneously measuring ^{62}Ni/^{60}Ni isotope ratios.

226   Samples were generally introduced in the plasma torch using a quartz spray
227   chamber equipped with Teflon nebulizer (50 μl/min). In some cases, increased instrument
228   sensitivity was required and the analyses were performed using X-cones. Under these
229   conditions, sample solutions were measured with concentrations ranging from 0.5 to 3
230   ppm. In all cases, the samples were diluted with 2% optima HNO_3 in appropriate
231   concentrations so that the IRMM-014 bracketing standards had the same concentration as
232   the sample. Potential ^{54}Cr interference was monitored by measuring ^{52}Cr intensity using
233   peak jumping in medium resolution mode to avoid $^{40}Ar^{12}C$ interferences.

234   Because instrumental mass bias is sensitive to matrix effects, we measured Mg and Ca
235   concentrations prior to isotope measurements. The aim is to quantify the efficiency of the
236   purification scheme by measuring elements present in seawater matrix. In all cases, we
237   verified that matrix elements were <1% of the total Fe concentration. Because Fe
238   isotopes can be fractionated during column chromatography (Anbar et al., 2000), we also
239   verified the yield of the purification step. For each sample, the matrix solution eluted from
240   the anion-exchange resin was collected in Teflon vials, evaporated and then analyzed by
241   spectrophotometry using the ferrozine method. In all cases, the loss of iron during the
242   purification step is less than 1%.

243   All analyses are reported in delta notation relative to the IRMM-014 standard,
244   expressed as δ^{56}Fe, which represents the deviation in per mil relative to the reference
245   material:

246   $$\delta^{56}Fe(\%_{oo}) = \left(\frac{(^{56}Fe/^{54}Fe)_{sample}}{(^{56}Fe/^{54}Fe)_{IRMM-014}} - 1 \right) \times 1000 \qquad (1)$$

247   We also reported δ^{57}Fe values but, since the relationships between δ^{56}Fe and δ^{57}Fe
248   of the samples plot on a single mass fractionation line, only δ^{56}Fe values are discussed in
249   this paper.

250   In order to check the accuracy of our Fe-isotope analyses in estuarine waters,

251   natural seawater matrices were doped with IRMM-014 standard and processed through

252   the complete chemistry steps as unknown samples. Duplicated purification and analysis

253   gave an average of δ^{56}Fe = 0.01 ‰ (2 σ = 0.06 ‰) for 17 samples which compared well

254   with pure standard processed through chemistry (in 18mΩ H_2O). The average Fe blank

255   measured in seawater matrices processed through chemistry was 10 ng, which

256   corresponds to about 0.1 % for the water samples and 0.01 % of the filters.

257

258   **4. Results**

259   *4.1. River end-member composition*

260   The river water end-member concentration of dissolved iron during the Oct. 2006

261   sampling of the estuary is 7.0 μM (**Table 1**). The sampling of the upstream river site on

262   Nov. 2007 (sample NR2) yielded 8.7 and 8.8 μM of dissolved Fe using cartridge and

263   membrane filtering methods (**Table 3**). The Mullica and Connecticut River yielded

264   dissolved Fe concentrations of 8.3 μM and 1.4 μM respectively (**Table 4**). Hence, the

265   two highly colored and organic-rich rivers contained significantly more dissolved Fe than

266   the Connecticut River.

267   Filtering a North River water sample through 0.22, 0.1, 0.05 and 0.025 μm pore-size

268   membranes lead to similar concentrations of Fe (8.8, 8.7, 8.3 and 8.7 μM respectively,

269   **Table 3**). While our filtration scheme was designed to remove colloidal Fe from the river

270   water sample, filtration down to a nominal pore size of 0.025 μm didn't remove colloidal

271   Fe (**Table 3**). Likewise, the Fe retained by the 0.1 and 0.025 μm pore-sized filters was

272   very low (0.08 μM) with respect to all four filtered fractions (~8.7 μM) and to the particle

273   (> 0.22 μm) Fe fraction (3.17 μM). Hence, the Fe retained by 0.1 and 0.025 μm filters

274   represents less than 1% of the total dissolved (<0.22 μm) Fe pool. Only the Fe retained

275   between the 0.22 and 0.05 μm fractions contained a significantly amount of Fe (0.47 μM).

276   Again, this Fe only represents 5% of the fraction of Fe passing through the four different

277   filter sizes. Hence, both the filtered and retained Fe for the pore-size study show that

278   filtration down to 0.025 μm was not small enough to remove colloidal Fe from the river

279   water of the North River. As discussed in the next section, there is large (83%) removal

280   of dissolved (<0.22 μm) Fe in the North River estuary. This removal is almost certainly

281   due to the salting-out of river Fe colloids. Hence, the colloids removed during estuarine

282   mixing must be smaller in size than 0.025 μm.

9

283

284   The isotopic Fe composition of three filtered (<0.22 μM) NR2 river water samples

285   displays positive δ^{56}Fe values of similar magnitude relative to IRMM-014 standard.

286   These values are 0.37, 0.34 and 0.38‰ (**Tables 1 and 3**). These values are also ~0.3‰

287   heavier than the bulk Earth value defined at 0.09‰ relative to IRMM-14 (Beard et al.,

288   2003a; Dauphas and Rouxel, 2006). In contrast, the total particulate Fe fraction (>0.22

289   μm) of upstream river site had the most negative δ^{56}Fe value at -0.22‰ (**Table 3**). The

290   two lowest salinity samples of the estuarine transect also had negative δ^{56}Fe value at -0.09

291   and -0.01‰ Hence, the difference between dissolved and particulate Fe in North River is

292   about 0.5‰ (+ 0.37 vs. -0.1‰).

293   Iron passing through 0.22 μm to 0.025 μm filter pore size show negligible variations

294   in Fe-isotope compositions (average δ^{56}Fe of 0.39 ± 0.04‰). As noted above, these four

295   filtrates also show little variation in their dissolved Fe concentrations (~8.3-8.8 μM). The

296   Fe fractions retained by the 0.1, 0.05 and 0.025 μm pore-sized filters (starting with the

297   <0.22 μm filtrate) are characterized by a δ^{56}Fe composition of -0.12, 0.14 and 0.09 ‰

298   respectively.   These 'colloidal'' values are more positive than the river (>0.22 μm)

299   particles at -0.22‰ but lower than all four filtrates (< 0.22 down to <0.025 μm) at 0.34 to

300   0.44 ‰ (**Table 3**). As noted above, our size-filtering scheme yields little in the way of

301   colloidal Fe. Hence, our pore-size study was not able to directly characterize the Fe

302   isotopic composition of the major pool of river colloids in the North River. Ultrafiltration

303   techniques are part of on-going project to isolate the pool of Fe colloids.

304

305   *4.2. Element behavior in North River estuary*

306   The estuarine distributions of dissolved (<0.22 μm) Fe and Al along the salinity

307   gradient of North River estuary show that both elements deviate markedly from

308   conservative mixing with very similar shapes (**Fig. 2**). The salinity distribution of

309   dissolved Fe and Al remain similar under ebb and flood tides conditions. Hence, we will

310   consider the two transects as one. This observation also permits us to assume that iron

311   precipitation is only salinity-dependant.

312   Large scale net removal of dissolved Fe during estuary mixing in the North River is a

313   common feature of estuaries (Boyle et al., 1977; Sholkovitz et al., 1978; Mayer, 1982;

314   Fox and Wofsy, 1983; Forsgren et al., 1996; Hunter et al., 1997; Gustafsson et al., 2000).

315   Though much less studied than Fe, field results confirm that the non-conservative removal

316   pattern of Al does occur in estuaries (Hydes and Liss, 1977; Crerar et al., 1981;

317   Upadhyay, 2008). Ultrafiltration studies (Ross and Sherrell, 1999) and laboratory-based

318   experiments (Eckert and Sholkovitz, 1976) also show that dissolved Al in organic rich

319   rivers exists as humic-type colloid and undergoes extensive salt-induced flocculation.

320

321   The percentage of Fe removal during estuarine mixing has been calculated following

322   the flux model of Boyle et al. (1974). The explicit formulation of this mixing model

323   implies that, over straight-line segments of the curve, simple two end-member dilution

324   processes can be considered. Using this approach, pure river and seawater end-members

325   as well as the percentage removal of Fe can be determined. Because the salinity along

326   North River estuary ranges from 0.2 to 30, we can extrapolate our measured dissolved Fe

327   concentrations at low salinity (i.e. S between 0.2 and 5) to derive the Fe concentration for

328   the river water end-member as 7.5μM. Similarly, we can extrapolate our measured

329   dissolved Fe concentrations at high salinity (i.e. S between 20 and 30) to derive the Fe

330   concentration at the zero-salinity intercept as 1.4μM (**Table 4**). The removal of Fe due to

331   the flocculation process is then estimated by the difference between the initial Fe

332   concentration in the river end-member and the Fe concentration at the zero-salinity

333   intercept. The model results yield a net removal of 83% for dissolved Fe in North River

334   estuary; this value compares well with other estuaries in the northeast United States

335   (Boyle et al., 1977). The net removal for dissolved Al is also large ~ 85%. Color can

336   serve as a semi-quantitative proxy of dissolved humic substances (Eckert and Sholkovitz,

337   1976; Sholkovitz, 1976). **Figure 2** shows there is small, but significant, amount of

338   removal of dissolved humic compounds (i.e. color) from the river water during estuarine

339   mixing. The color removal, based on the salinity distribution model of Boyle et al. (1974)

340   is ~ 30%. As expected, the results show a linear relationship between Ca and Mo with

341   salinity, consistent with conservative behavior during estuarine mixing.

342   The distribution of particulate Fe concentration vs. salinity is presented in **Figure 3**

343   and display a sharp decrease at low salinity, from 7 μM in the river end-member down to

344   3 μM at salinity of 5. The ratio of dissolved Fe relative to particulate Fe (**Figure 3**)

345   indicates that approximately 45 to 50% of the total Fe in North River is carried in the

346   dissolved load. This proportion decreases to less than 5% at the high-salinity end of the

347   estuary.

348

11

349   *4.3. Determination of the flocculation factor*

350   In order to relate potential Fe-isotope fractionation during the flocculation process, we

351   calculated the fraction (F) of dissolved Fe removed in each sample along the salinity

352   gradient. F is calculated using the ratio of measured Fe concentration corrected from

353   seawater mixing, *versus* the initial dissolved Fe concentration in the river (i.e. freshwater)

354   end-member, such as:

355
$$F = 1 - \left(\frac{Fe_{SW}}{Fe_{RW}} + \frac{Fe_S - Fe_{SW}}{Fe_{RW}} \times \frac{1}{1 - S/35} \right) \qquad (2)$$

356   Where Fe_{SW} is the concentration of Fe in the seawater end-member (less than 0.01

357   μM), Fe_s the measured concentration at the salinity S, and Fe_{RW} the concentration in the

358   river end-member (7.5 μM). Although the concentration of dissolved Fe in local coastal

359   seawater has not been determined, total dissolved Fe concentrations of about 10 nM have

360   been already reported in surface seawater of Massachusetts Bay by Zhuang et al. (1995).

361   Because end-member seawater Fe concentrations represent less than 1% of the initial Fe

362   from the river, using seawater Fe concentrations of up to 20nM, as found in other local

363   coastal seawater (Rouxel, 2009) has no effects on the value of F. As presented in **Figure**

364   **4**, the fraction of Fe removed by colloid flocculation shows a drastic increase up to 0.5

365   below a salinity of 5 then increases slowly up to 0.7 for a salinity of 10. At higher salinity,

366   the percentage of flocculated iron is relatively stable between 70 to 80%. The Fe-isotope

367   compositions of both particulate and dissolved Fe pools along the salinity gradient of

368   North River estuary are presented in **Table 2** and **Figure 5**. The dissolved Fe pool (i.e. <

369   0.22 μm fraction) does not display any systematic changes in δ^{56}Fe values along the

370   estuary and yields an average Fe-isotope composition of 0.43 $\pm$ 0.04‰. In contrast,

371   particulate Fe-isotope compositions increase from -0.1 to 0.15‰ between salinities of 0.2

372   to ~5‰. At higher salinities, suspended particles yield δ^{56}Fe values similar, within

373   uncertainties, to crustal materials defined at 0.09‰ (Rouxel et al., 2003; Beard et al.,

374   2003a,b).

375

376   **5. Discussion**

377

378   *5.1. Fe-isotope systematics in colloidal and particulate pools in the river end member*

379   An important result of this study is that the dissolved Fe fraction of North River

380   has a positive δ^{56}Fe value of ~0.4‰ which is heavier than the crustal composition defined

381   at ~0.09‰ and heavier than most previous studies in other riverine systems (Fantle and

382   DePaolo, 2004; Bergquist and Boyle, 2006; Ingri et al., 2006). Another important result is

383   the significant differences in Fe-isotope compositions between the dissolved and

384   particulate iron in the riverine end-member. This difference reaches 0.46‰ and 0.60‰ in

385   North River sampled in October and November 2006 respectively.

386   Although Fantle and DePaolo (2004) analyzed unfiltered river water, they

387   proposed that soluble Fe in rivers is characterized by more negative δ^{56}Fe values

388   compared to the average crust (i.e. δ^{56}Fe values between -0.78 to 0.13‰ for 8 rivers from

389   North America). Bergquist and Boyle (2006) reported δ^{56}Fe composition of filtered (<0.4

390   μm) Amazon River waters showing negative value (from -0.46 to -0.08‰) while the

391   Negro River water displayed heavier Fe-isotope composition (from 0.2 to 0.44‰). In

392   another study of Fe-isotope composition of suspended matter in a Boreal river in Sweden,

393   Ingri et al., (2006) proposed that Fe (III) – humic acid complexes represent a light pool of

394   iron isotopes in river colloids while Fe hydroxides would yield higher δ^{56}Fe values.

395   Altogether, with the exception of the Rio Negro, most previous studies are consistent with

396   the preferential loss of light Fe-isotopes during weathering and mineral dissolution

397   processes (Brantley et al., 2004; Thompson et al., 2007). However, the hypothesis that

398   organically-bound Fe in rivers can be characterized by lighter Fe-isotope composition is at

399   odd with the enrichment in heavy Fe isotopes in river colloids at North River. In

400   particular, the Fe-isotope analysis of various size fraction of colloids at North River

401   (**Table 3**) suggests that the larger colloidal fraction (e.g. >0.025 μm) are lighter by up to

402   0.3‰ relative to finer colloids (e.g. <0.025 μm). Hence, these results confirm that

403   colloids, probably composed of Fe(III)-humic or other organic ligand complexes, yield

404   positive δ^{56}Fe values relative to suspended sediments.

405   The Connecticut and Mullica rivers yielded δ^{56}Fe values of 0.18 ‰ and -0.33 ‰

406   respectively. This large variation between these two rivers suggest that the value of iron

407   isotope is not principally controlled by the organic content in the water: the Connecticut

408   River, which represents a large mineral discharge of North East America, has lower

409   content of dissolved humic compounds than North River but has slightly lower δ^{56}Fe

410   values. Hence, the high value δ^{56}Fe for North River is at odds with the expectation that

411   Fe-C compounds are characterized by lighter Fe-isotope composition. Only Mullica

412   River, which is characterized by the highest organic matter content and Fe concentration

413   (Sholkovitz, 1976; Crerar et al., 1981; Yan et al., 1990) is characterized by lower δ^{56}Fe

13

414 values than crustal material may be consistent with the preferential partitioning of light
415 Fe-isotopes with organic compounds.

416   In principle, Fe isotopes variability in rivers can be related to the mineralogy of the
417 rocks and sediments present in watersheds, the weathering regime (chemical vs. physical
418 erosion), and the presence of ligands during weathering (Brantley et al., 2004; Fantle and
419 DePaolo, 2004). In addition, changes in iron isotopes composition can also be linked to
420 biological (Johnson et al., 2004) and chemical processes such as adsorption (Icopini et al.,
421 2004; Teutsch et al., 2005), precipitation (Skulan et al., 2002), and redox conditions
422 (Severmann et al., 2006; Rouxel et al., 2008b).

423   Although the Fe isotope composition of the upper continental crust has been
424 recently debated in the literature (Poitrasson and Freydier, 2005; Beard and Johnson,
425 2006; Poitrasson, 2006), numerous evidences suggest that sedimentary clastic rocks have
426 average δ^{56}Fe value similar to igneous rocks. Only a limited number of high-SiO_2 granitic
427 rocks (δ^{56}Fe up to 0.4‰) have been shown to deviate from the igneous average. However,
428 those crustal components have likely a minimal impact on the global composition of the
429 continental crust. Hence, it is unlikely that the high- δ^{56}Fe values of dissolved Fe observed
430 at North River is due to the weathering of isotopically heavy rocks.

431   Among other processes, the precipitation or adsorption of isotopically light Fe
432 onto riverine particles may also explain positive δ^{56}Fe values in the dissolved pool. The
433 observation that suspended particulate matter in North River has δ^{56}Fe values ~0.5‰
434 lower than the dissolved pool is consistent with this hypothesis. Similar to North River,
435 the Negro River in the Amazon system, which displays heavier Fe-isotope composition
436 (up to 0.44‰) for dissolved Fe, has particulates up to ~ 1.2 ‰ lighter than the associated
437 dissolved Fe. We also note that similar results have been already reported for other
438 isotope systems such as Li (Huh et al, 2001) and Cu (Vance et al, 2008) isotopes. In
439 particular, heavier Cu-isotope compositions of the dissolved phase relative to the
440 particulate Cu-pool have been interpreted as resulting from an equilibrium isotope effects.
441 The process of Fe-isotope fractionation between dissolved and particulate pools remains,
442 however, unclear as the nature of Fe-species involved is unknown. Approximately half of
443 the total Fe in North River is carried in the dissolved load (**Figure 3**). Hence, the δ^{56}Fe
444 value for total Fe is ~ 0.1‰ which is similar to the bulk crust value. This suggests that the
445 total Fe-isotope composition in the riverine system is not significantly fractionated by
446 continental run-off but that the production of colloidal organic species may produce

447 significant Fe-isotope fractionation between particulate and colloidal pools. Recent
448 experimental studies of isotope fractionation between organically bound and inorganic
449 Fe(III) species in solution are consistent with this hypothesis. Dideriksen et al., (2008)
450 found that Fe(III) bound to strongly coordinating ligands is likely to yield heavier δ^{56}Fe
451 values (up to 0.6‰) than the inorganically complexed Fe, which may be removed from
452 solution through precipitation. In the case of North River, similar isotope effects may
453 occur: the preferential removal of isotopically light inorganic dissolved Fe (e.g. Fe-oxide
454 and clays) may leave the dissolved - organically complexed – colloidal pool enriched in
455 heavy isotopes. Alternatively, in the North River estuary, high concentration of dissolved
456 humic substances may provide stronger bonding environments than Fe-hydroxide- or
457 clay-rich particules. In this case, heavier Fe-isotope composition in the dissolved Fe pool
458 may result from direct Fe-isotope fractionation between dissolved and particulate pools,
459 whereby heavy isotopes are partitioned preferentially in the stronger bonding
460 environments (Urey, 1947 and Schauble, 2004), as recently observed for Cu-isotopes
461 (Vance et al, 2006). Additional studies of Fe-speciation in rivers (e.g. Gledhill and Van
462 den Berg, 1995) combined with Fe-isotope composition may solve this issue.
463 An alternate hypothesis is that the heavy δ^{56}Fe values in rivers are generated during the
464 preferential retention of light Fe-isotopes in soils, either through secondary mineral
465 precipitation (e.g. Wiederhold et al., 2007) or plant uptake (Guelke and Von
466 Blanckenburg, 2007). The fact that both dissolved and particulate pools in the North River
467 has Al/Fe ratios lower than crustal values (Al/Fe~0.15 vs Al/Fe~1.5, **Figure 6**) is
468 consistent with incongruent weathering and formation of (Fe,Al)-silicates in soils.
469 However, it is presently unclear if the Fe-isotopic difference between dissolved and
470 particulate phases may be influenced by weathering intensity as previously reported for Li
471 isotopic system (Huh et al, 2001).
472
473   *5.2. Fe-isotope systematics of dissolved Fe during flocculation process in estuaries*
474 Dissolved Fe has long been recognized as having a non-conservative behavior in most
475 estuaries (Boyle et al., 1977; Sholkovitz et al., 1978; Bale and Morris, 1981; Mayer, 1982;
476 Fox and Wofsy, 1983; Forsgren et al., 1996; Hunter et al., 1997; Gustafsson et al., 2000).
477 It is generally assumed that the coagulation of Fe-rich colloids results from the
478 destabilization of organic complexes and negatively charged-Fe colloids by seawater
479 cations. In this study, we have shown that most dissolved Fe in North River is affected by
480 large-scale removal at low salinity (<15‰), reducing the effective input of dissolved Fe to

481   the ocean by about 83% of the primary river value. The precipitation of organic-rich

482   riverine colloids at North River is also confirmed by the non-conservative behavior of

483   humic compounds (i.e. color) distribution along the estuary and by the removal of Al

484   (**Figure 3**), which is also closely associated with organic material (Eckert and Sholkovitz,

485   1976). Since the coagulation of Fe-humic colloids involves complex transformations

486   between labile, colloidal and particulate phases, estuaries may modify the isotopic

487   composition of riverine source of Fe to the oceans in the following cases:

488   (1) If chemical weathering results in river water having humic-Fe colloids with a

489   different isotopic composition than soluble Fe, then estuarine flocculation should lead to

490   modification of Fe isotope composition of dissolved Fe, reflecting the preferential

491   removal of colloids relative to labile Fe which are not affected by flocculation. At North

492   River, soluble Fe (i.e. pool of dissolved Fe which is not affected by flocculation process)

493   represents about 20% of the total dissolved Fe concentration, **Table 4**. The evolution of

494   dissolved δ^{56}Fe values relative to the amount F of Fe precipitated can be described by the

495   mass balance equation:

496    $$(1-F) \times \delta^{56}Fe = (F_{max} - F) \times \delta^{56}Fe_{col} + (1 - F_{max}) \times \delta^{56}Fe_{sol} \qquad (3)$$

497   Where F_{max} is the maximum extent of Fe precipitation in the estuary (determined at 0.83),

498    $\delta^{56}Fe_{col}$ and $\delta^{56}Fe_{sol}$ are the Fe-isotope composition of colloidal and soluble Fe end-

499   members. Note that this model does not include the potential contribution of seawater-

500   derived Fe which is estimated to be less than 0.01 μM, and thus negligible relative to river

501   borne Fe, even at the maximum salinity in North River estuary. Based on the relationship

502   between δ^{56}Fe and 1/(1-F) presented in **Figure 7**, the δ^{56}Fe difference between colloidal

503   Fe and labile Fe (calculated at F=0.9) is restricted to less than 0.14‰ ±0.15 (2SE) and

504   thus insignificant compared to the uncertainty (i.e. after error propagation).

505   (2) If significant Fe isotope fractionation occurs between particulate and dissolved

506   Fe, then estuarine mixing should lead to isotope fractionation during Fe removal. Because

507   colloids offer a much greater number of surface complexation sites than suspended

508   particles, potential exist for isotope fractionation during adsorption processes or during

509   precipitation/aggregation of colloids onto suspended particles. In this case, the

510   precipitation of humic-Fe colloids corresponds to a unidirectional process (i.e. no further

511   reactions between dissolved and particulate Fe pools), the fraction F of Fe precipitated, as

512   defined in equation (2), and the Fe-isotope composition in the remaining dissolve pool

513   can be determined by the Rayleigh law:

514
$$\delta^{56}Fe = (1000 + \delta^{56}Fe_0) \times (1-F)^{(\alpha-1)} - 1000 \quad (4)$$

515 where $\delta^{56}Fe_0$ is the initial value of the river end-member and α is the particulate-dissolved

516 fractionation factor during the flocculation process. Using this relationship, it is possible

517 to calculate the maximum α values producing the distribution of $\delta^{56}Fe$ values along the

518 estuary (**Figure 7**). Since $\delta^{56}Fe$ values of the estuarine samples are identical within

519 uncertainties, α equal to 0.99993 ± 0.00006 (2SE) which implies that Fe-isotope

520 fractionation during the flocculation processes is less than 0.07‰ and does not

521 significantly affect the iron isotopes of rivers within uncertainty.

522

523 *5.3. Fe-isotope systematics in the particulate pool*

524 Iron in suspended particles (>0.22 μm) is essentially associated with clays, humic

525 compounds and Fe oxides (e.g. Ross and Sherrell, 1999; Poulton and Raiswell, 2002;

526 Allard et al., 2004). In estuaries, newly formed particles due to colloid flocculation are

527 expected to represent another important pool of Fe. Although suspended particles in North

528 River are characterized by sub-crustal $\delta^{56}Fe$ values around -0.1‰, the precipitation of

529 isotopically heavy colloids should result in significant alteration (i.e. increase) of $\delta^{56}Fe$

530 values of estuarine particles. As illustrated in **Figure 2 and 6**, dissolved Al behaves

531 similarly to Fe in the estuary (i.e. non-conservative behavior) with Al/Fe being constant

532 over a wide range of salinity. In contrast, Al/Fe ratios in suspended particles display a

533 gradual increase with salinity, from dissolved Al/Fe ratios of ~ 0.15 (g/g) in the

534 freshwater end-member to sub-crustal values ~ 1.6 (g/g) at high salinity. Consequently,

535 particulate Al/Fe ratios cannot be explained by a simple binary mixing between river-

536 borne particles and newly formed particles due to colloid flocculation. A third Fe

537 component needs to be taken in consideration, that is, lithogenic particles with near

538 crustal Al/Fe ratios. This last source corresponds to a major part of suspended marine

539 sediments with an assumed Al/Fe ratios of ~ 2.0 (g/g) and crustal $\delta^{56}Fe$ (=0.09 ‰)

540 consistent with upper continental crust values (Dauphas and Rouxel, 2006; Rudnick and

541 Gao, 2007).

542 From the relationship between $\delta^{56}Fe$ and Al/Fe values in estuarine particles

543 (**Figure 8**), we can define 3-component mixing relationships such as:

544 $$\delta^{56}Fe_{part} = X_{RP} \times \delta^{56}Fe_{RP} + X_{Col} \times \delta^{56}Fe_{Col} + X_{Lith} \times \delta^{56}Fe_{Lith} \quad (5)$$

545 $$(Al/Fe)_{part} = X_{RP} \times (Al/Fe)_{RP} + X_{Col} \times (Al/Fe)_{Col} + X_{Lith} \times (Al/Fe)_{Lith} \quad (6)$$

17

546   where X_{RP}, X_{Col} and X_{Lith} correspond to the fraction of Fe in estuarine particles

547   (*part*) derived from river-borne particles (*RP*), flocculated colloids (*Col*) and lithogenic

548   particles (*Lith*) respectively. These values can be determined for each estuarine sample

549   using the equations (5-6) which can be simplified considering that Al/Fe ratios in river-

550   borne particles and colloids are similar, such as:

551    $$X_{Lith} = \left[(Al/Fe)_{part} - (Al/Fe)_{RP}\right] / \left[(Al/Fe)_{Lith} - (Al/Fe)_{RP}\right] \quad (7)$$

552    $$X_{Col} = \frac{\delta^{56}Fe_{RP} - \delta^{56}Fe_{part}}{\delta^{56}Fe_{RP} - \delta^{56}Fe_{Col}} - X_{Lith} \frac{\delta^{56}Fe_{RP} - \delta^{56}Fe_{Lith}}{\delta^{56}Fe_{RP} - \delta^{56}Fe_{Col}} \quad (8)$$

553    $$X_{RP} = 1 - X_{Col} - X_{Lith} \quad (9)$$

554   The mixing relationships between these three components are illustrated in **Figure 8a**

555   showing $\delta^{56}Fe$ *vs.* Al/Fe ratios of dissolved Fe (<0.22 μm) and particulate Fe (>0.22 μm)

556   along the North River estuary. The most striking feature is the increase of X_{Lith} with

557   increasing salinity (**Figure 8b**). This suggests that lithogenic particles derived from local

558   seawater end-member, probably through sediment resuspension along the coastal zone. In

559   particular, the high-energy environments provided by coastal seawaters may carry

560   significant suspended sediments that can mix with estuary particles. Although an increase

561   of X_{Col} is observed at low salinity (S<5) due to flocculation process as river water mixes

562   with seawater, the decrease of X_{Col} at higher salinity is more surprising. As mentioned

563   previously, the Al/Fe ratios in suspended particles (i.e. X_{Lith}) display a gradual increase

564   with salinity which result in relative decrease of riverine particles and colloids in the

565   estuary. In **Figure 9**, the relationship between X_{Col}/X_{RP} and the flocculation factor (*F*)

566   reveals a positive correlation with a slope close to unity (0.9 ± 0.1). As illustrated in

567   **Figure 3**, approximately 45 to 50% of the total Fe in North River is carried in the

568   dissolved load. Hence, the total fraction of colloidal Fe relative to river-borne particulate

569   Fe, will be about 0.8 to 0.95 after quantitative flocculation (i.e. F=1). Hence, both

570   independent approaches are in good agreement which confirms that only river-seawater

571   mixing process and colloid flocculation control dissolve and particulate Fe concentration

572   in North River estuary. In contrast, such processes have essentially no effect of Fe-isotope

573   composition of dissolved Fe.

574

575   *5.4. Implication for coastal seawater Fe sources*

576

577   Among important sources of iron in coastal seawater, diagenetic pore fluids from
578 shelf sediments (Staubwasser et al., 2006; Bergquist et Boyle, 2006; Severmann et al.,
579 2006; 2008) and groundwater (Rouxel et al., 2008b) have been suggested to provide
580 significant source of low- δ^{56}Fe iron to the oceans. Based on the observed homogeneity of
581 Fe isotope composition of suspended loads of major rivers across the United States, it has
582 been initially suggested that Fe inputs to the ocean via rivers is similar to igneous rocks
583 (Beard et al., 2003b). However, later studies have suggested that continental run-off may
584 represent another source of low- δ^{56}Fe iron in coastal waters (Bergquist and Boyle, 2006;
585 Fantle and De Paolo, 2004; Ingri et al, 2006). Suspended load may have also δ^{56}Fe values
586 fractionated towards negative values suggesting that Fe isotope composition of river-
587 borne particles is not unique (Bergquist and Boyle, 2006, this study). Since the process of
588 flocculation produces minimal Fe-isotope fractionation in the dissolved Fe pool, we
589 suggest that the Fe isotope composition of dissolved Fe in rivers is preserved during
590 estuarine mixing and that the global riverine source into the ocean can display both
591 heavier and lighter δ^{56}Fe values (between -0.5 to up to 0.3 per mil) relative to the
592 continental crust. Since different river types may have different colloid size and
593 compositions that may behave differently than the North River, the total range of Fe-
594 isotope composition of the worldwide rivers is still poorly known.

595   Despite those uncertainties, our study suggests that dissolved riverine Fe can be
596 characterized by near crustal or slightly positive δ^{56}Fe values which contrast strongly with
597 benthic Fe sources having strongly negative δ^{56}Fe values due to suboxic Fe cycling
598 (Severmann et al., 2006; Rouxel et al., 2008b). Hence, Fe-isotopes can provide valuable
599 tracers to distinguish various Fe-sources in coastal oceans and their potential impact in
600 marine ecosystems. This hypothesis is consistent with a recent study of the 100 km long
601 Scheldt estuary (de Jong et al., 2007) where negative δ^{56}Fe values down to −1.2‰ have
602 been observed along a salinity gradient. The occurrence of low δ^{56}Fe values for dissolved
603 Fe in the Scheldt estuary has been attributed to either Fe-isotope fractionation processes
604 due to redox cycling in the estuary or from adsorption/precipitation of dissolved Fe onto
605 particulate matter. Based on our study, it can be suggested that low δ^{56}Fe values in the
606 Scheldt estuary result from the contribution of an additional Fe source, probably derived
607 from the diffusive input of isotopically light Fe from anoxic estuary sediments.   The
608 potential addition of groundwater-derived Fe may also produce such negative Fe-isotope
609 signature, as already observed in Waquoit Bay (Rouxel et al., 2008b; Rouxel 2009).

610

6. Conclusion

611

612

613   The major objective of this study was to determine the processes controlling the

614   fractionation of Fe isotopes between continental run-off and the oceans. The main

615   findings are:

616   (1) Continental run-off yields colloidal Fe pools in rivers that are isotopically distinct

617   from particulate Fe pools. In particular, we demonstrated that the particulate and dissolved

618   fractions in a small river in North Eastern US are characterized by a difference of Fe–

619   isotopic composition of up to 0.5‰ which is almost 10 times the analytical uncertainty.

620   The particulate fraction (>0.22 μm) yields negative δ^{56}Fe values while the dissolved

621   fraction <0.22 μm yielded positive δ^{56}Fe values relative to the bulk continental crust.

622   (2) The large scale removal of river-borne dissolved Fe, a universal feature of

623   estuaries, does not significantly modify the Fe isotopic signature of terrestrial dissolved

624   Fe reaching coastal waters. This suggests that, although Fe has a distinctly non-

625   conservative behavior in estuaries, the δ^{56}Fe composition of rivers is not modified in

626   estuaries. Based on Al/Fe and Fe-isotope ratios, we also determined that the suspended

627   pool along the North River estuary is controlled by the relative proportion of river-borne

628   particles, coagulated river colloids and detrital Fe derived from coastal area.

629   These results contrast with previous finding suggesting mostly negative δ^{56}Fe values

630   for dissolved Fe in rivers (Fantle and DePaolo, 2004; Bergquist and Boyle, 2006). The

631   oceanic input of Fe from rivers could have a local influence on the iron composition of the

632   costal ocean which can be distinguished from diagenetic input from marine sediment and

633   groundwater, the later having essentially negative δ^{56}Fe values (Severmann et al., 2006;

634   Rouxel et al., 2008b). Hence, Fe-isotopes provide valuable tracers of Fe-sources in

635   hydrologic and marine environments. Additional work is now required to assess the

636   importance of weathering regime and climate on the temporal and spatial variability of Fe

637   isotope composition of rivers.

638

639

640

641

649

650

651

652

References

Allard, T., Menguy, N., Salomon, J., Calligaro, T., Weber, T., Calas, G., and Benedetti, M. F., 2004. Revealing forms of iron in river-borne material from major tropical rivers of the Amazon Basin (Brazil). *Geochimica et Cosmochimica Acta* **68**, 3079-3094.

Anbar, A., 2003. Iron stable isotopes: beyond biosignatures. *Earth Planet. Sci. Lett.* **217**, 223-236.

Anbar, A. D., Roe, J. E., Barling, J., and Nealson, K. H., 2000. Nonbiological Fractionation of Iron Isotopes. *Science* **288**, 126-128.

Archer, D. E. and Johnson, K., 2000. A model of the iron cycle in the ocean. *Global Biogeochemical Cycles* **14**, 269-279.

Bale, A. J. and Morris, A. W., 1981. Laboratory simulation of chemical processes induced by estuarine mixing: the behavior of iron and phosphate in estuaries. *Estuarine Coastal Shelf Sci.* **13**, 1-10.

Beard, B. L. and Johnson, C. M., 2004. Fe isotope variations in the modern and ancient Earth and other planetary bodies. *Reviews in Mineralogy and Geochemistry* **55**, 319-357.

Beard, B. L. and Johnson, C. M., 2006. Comment on "Heavy iron isotope composition of granites determined by high resolution MC-ICP-MS", by F. Poitrasson and R. Freydier [Chem. Geol. 222 132-147]. *Chemical Geology* **235**, 201-204.

Beard, B. L., Johnson, C. M., Skulan, J. L., Nealson, K. H., Cox, L., and Sun, H., 2003a. Application of Fe isotopes to tracing the geochemical and biological cycling of Fe. *Chemical Geology* **195**, 87-117.

Beard, B. L., Johnson, C. M., VonDamm, K. L., and Poulson, R. L., 2003b. Iron isotope constraints on Fe cycling and mass balance in oxygenated Earth oceans. *Geology* **31**, 629-632.

Bennett, S. A., Achterberg, E. P., Connelly, D. P., Statham, P. J., Fones, G. R., and German, C. R., 2008. The distribution and stabilisation of dissolved Fe in deep-sea hydrothermal plumes. *Earth Planet. Sci. Lett.* **270**, 157-167.

Bergquist, B. and Boyle, E., 2006. Iron isotopes in the Amazon river system: weathering and transport signatures. *Earth Planet. Sci. Lett.* **248**, 54-68.

Boyd, P. W., Watson, A. J., Law, C. S., Abraham, E. R., Trull, T., R.Murdoch, Bakker, D. C. E., Bowie, A., Buesseler, K. O., Chang, H., Charette, M., Croot, P., Downing, K., Frew, R., Gall, M., Hadfield, M., Hall, J., Harvey, M., Jameson, G., DeLaRoche, J., Liddicoat, M., Ling, R., Maldonado, M. T., McKay, R. M., Nodder, S., Pickmere, S., Pridmore, R., Rintoul, S., Safi, K., Sutton, P., Strzepek, R., Tanneberger, K., Turner, S., Waite, A., and Zeldis, J., 2000. A mesoscale phytoplankton bloom in the polar Southern Ocean stimulated by iron fertilization. *Nature* **407**, 695-702.

Boyle, E., Collier, R., Dengler, A. T., Edmond, J. M., Ng, A. C., and Stallard, R. F., 1974. On the chemical mass-balance in estuaries. *Geochimica et Cosmochimica Acta* **38**, 1719-1728.

Boyle, E. A., Bergquist, B. A., Kayser, R. A., and Mahowald, N., 2005. Iron, manganese, and lead at Hawaii Ocean Time-series station ALOHA: Temporal variability and an intermediate water hydrothermal plume. *Geochim. Cosmochim. Acta* **69**, 933-952.

Boyle, E. A., Edmond, J. M., and Sholkovitz, E. R., 1977. The mechanism of iron removal in estuaries. *Geochimica et Cosmochimica Acta* **41**, 1313-1324.

Brantley, B. L., Liermann, L. J., Guynn, R. L., Anbar, A., Icopini, G. A., and Barling, J., 2004. Fe isotopic fractionation during mineral dissolution with and without bacteria. *Geochim. Cosmochim. Acta* **68**, 3189-3204.

Brantley, S. L., Liermann, L., and Bullen, T. D., 2001. Fractionation of Fe isotopes by soil microbes and organic acids. *Geology* **29**, 535-538.

Christian, J. R., Verschell, M. A., Murtugudde, R., Busalacchi, A. J., and McClain, C. R., 2002. Biogeochemical modelling of the tropical Pacific Ocean. II: Iron biogeochemistry. *Deep-Sea Res. II* **49**, 545-565.

Gledhill, M. and van den Berg, C. M. G., 1994, Determination of complexation of iron(III) with natural organic complexing ligands in seawater using cathodic stripping voltammetry. *Marine Chemistry* 47(1): 41-54.

Crerar, D. A., Means, J. L., Yuretich, R. F., Borcsik, M. P., Amster, J. L., Hastings, D. W., Knox, G. W., Lyon, K. E., and Quiett, R. F., 1981. Hydrogeochemistry of the New Jersey coastal plain 2. Transport and deposition of iron, alumunium, dissolved organic matter, and selected trace elements in stream, ground- and estuary water. *Chemical Geology* **33**, 23-44.

Dauphas, N. and Rouxel, O., 2006. Mass spectrometry and natural variations of iron isotopes. *Mass Spectrometry Reviews* **25**, 515-550.

de Jong, J., Schoemann, V., Tison, J.-L., Becquevort, S., Masson, F., Lannuzel, D., Petit, J., Choua, L., Weis, D., and Mattielli, N., 2007. Precise measurement of Fe isotopes in marine samples by multi-collector inductively coupled plasma mass spectrometry (MC-ICP-MS). *Analytica Chimica Acta* **589**, 105-119.

Dideriksen, K., Baker, J. A., and Stipp, S. L. S., 2008. Equilibrium Fe isotope fractionation between inorganic aqueous Fe(III) and the siderophore complex, Fe(III)-desferrioxamine B. *Earth and Planetary Science Letters* **269**, 280-290.

Eckert, J. and Sholkovitz, E. R., 1976. The flocculation of iron, aluminum and humates from river water by electrolytes. *Geochimica et Cosmochimica Acta* **40**, 847-848.

Elderfield, H. and Schultz, A., 1996. Mid-ocean ridge hydrothermal fluxes and the chemical composition of the ocean. *Annu. Rev. Earth Planet. Sci.* **24**, 191-224.

Elrod, V. A., Berelson, W. M., Coale, K. H., and Johnson, K. S., 2004. The flux of iron from continental shelf sediments: A missing source for global budgets. *Gephysical Research Letters* **31**, doi:10.1029/2004GL020216.

Fantle, M. S. and DePaolo, D. J., 2004. Iron isotopic fractionation during continental weathering. *Earth Planet. Sci. Lett.* **228**, 547-562.

Forsgren, G., Jansson, M., and Nilsson, P., 1996. Aggregation and Sedimentation of Iron, Phosphorus and Organic Carbon in Experimental Mixtures of Freshwater and Estuarine Water. *Estuarine, Coastal and Shelf Science* **43**, 259-268.

Fox, L. E. and Wofsy, S. C., 1983. Kinetics of removal of iron colloids from estuaries. *Geochimica et Cosmochimica Acta* **47**, 211-216.

Garvine, R. W., 1975. The distribution of salinity and temperature in the Connecticut River Estuary. *Journal of Geophysical Research* **80**, 1176-1183.

Guelke, M. and vonBlanckenburg, F., 2007. Fractionation of Stable Iron Isotopes in Higher Plants. *Environ. Sci. Technol.* **41**, 1896-1901.

Gustafsson, O., Widerlund, A., Andersson, P. S., Ingri, J., Ross, P., and Ledin, A., 2000. Colloid dynamics and transport of major elements through a boreal river - brackish bay mixing zone. *Mar. Chem.* **71**, 1-21.

Huh, Y., Chan L.-H., and Edmond J., 2001. Lithium isotopes as a probe of weathering processes: Orinoco River. *Earth and Planetary Science Letters* 194(1-2): 189-199.

750 Hunter, K. A., 1990. Kinetics and mechanisms of iron colloid aggregation in estuaries. In:
751   Beckett, R. (Ed.), *Surface and Colloid Chemistry in Natural Waters and Water*
752   *Treatment*. Plenum Press, New York.
753 Hunter, K. A., Leonard, M. R., Carpenter, P. D., and Smith, J. D., 1997. Aggregation of
754   iron colloids in estuaries: a heterogeneous kinetics study using continuous mixing
755   of river and sea waters. *Colloids and Surfaces A: Physicochemical and*
756   *Engineering Aspects* **120**, 111-121.
757 Hydes, D. J. and Liss, P. S., 1977. The behavior of dissolved aluminum in estuarine and
758   coastal waters. *Estuarine and Coastal Marine Science* **5**, 755-769.
759 Icopini, G. A., Anbar, A. D., Ruebush, S. S., Tien, M., and Brantley, S. L., 2004. Iron
760   isotope fractionation during microbial reduction of iron: The importance of
761   adsorption. *Geology* **32**, 205-208.
762 Ingri, J., Malinovsky, D., Rodushkin, I., Baxter, D. C., Widerlund, A., Andersson, P.,
763   Gustafsson, Ö., Forsling, W., and Öhlander, B., 2006. Iron isotope fractionation in
764   river colloidal matter. *Earth and Planetary Science Letters* **245**, 792-798.
765 Jickells, T. D., An, Z. S., Andersen, K. K., Baker, A. R., Bergametti, G., Brooks, N., Cao,
766   J. J., Boyd, P. W., Duce, R. A., Hunter, K. A., Kawahata, H., Kubilay, N.,
767   laRoche, J., Liss, P. S., Mahowald, N., Prospero, J. M., Ridgwell, A. J., Tegen, I.,
768   and Torres, R., 2005. Global Iron Connections Between Desert Dust, Ocean
769   Biogeochemistry, and Climate. *Science* **308**, 67-71.
770 Johnson, C. M. and Beard, B. L., 2006. Fe isotopes: an emerging technique in
771   understanding modern and ancient biogeochemical cycles. *GSA Today* **16**, 4-10.
772 Johnson, C. M., Beard, B. L., Roden, E. E., Newman, D. K., and Nealson, K. H., 2004.
773   Isotopic constraints on biological cycling of Fe. *Reviews in Mineralogy and*
774   *Geochemistry* **55**, 359-408.
775 Johnson, K. S., Chavez, F. P., and Friederich, G. E., 1999. Continental-shelf sediment as a
776   primary source of iron for coastal phytoplankton. *Nature* **398**, 697-700.
777 Johnson, K. S., Gordon, R. M., and Coale, K. H., 1997. What controls dissolved iron
778   concentrations in the world ocean ? *Marine Chemistry* **57**, 137-161.
779 Lefevre, N. and Watson, A. J., 1999. Modeling the geochemical cycle of iron in the
780   oceans and its impact on atmospheric CO2 concentrations. *Global Biogeochemical*
781   *Cycles* **13**, 727-736.
782 Martin, J. H., 1990. Glacial-interglacial CO2 change: the iron hypothesis.
783   *Paleoceanography* **5**, 1-13.
784 Mayer, L. M., 1982. Retention of riverine iron in estuaries. *Geochim. Cosmochim. Acta*
785   **46**, 1003-1009.
786 Moore, J. K., Doney, S. C., Glover, D. M., and Fung, I. Y., 2002. Iron cycling and
787   nutrient-limitation patterns in surface waters of the World Ocean. *Deep-Sea Res. II*
788   **463-507**.
789 Moore, J. K., Doney, S. C., and Lindsay, K., 2004. Upper ocean ecosystem dynamics and
790   iron cycling in a global 3-D model. *Global Biogeochem. Cycles* **18**,
791   doi:10.1029/2004GB002220.
792 Plank, T. and Langmuir, C. H., 1998. The chemical composition of subducting sediment
793   and its consequences for the crust and mantle. *Chemical Geology* **145**, 325-394.
794 Poitrasson, F., 2006. On the iron isotope homogeneity level of the continental crust.
795   *Chemical Geology* **235**, 195-200.
796 Poitrasson, F. and Freydier, R., 2005. Heavy iron isotope composition of granites
797   determined by high resolution MC-ICP-MS. *Chemical Geology* **222**, 132-147.
798 Poulton, S. W. and Raiswell, R., 2002. The low-temperature geochemical cycle of iron:
799   from continental fluxes to marine sediment deposition. *Am. J. Sci.* **302**, 774-805.

800 Ross, J. M. and Sherrell, R. M., 1999. The role of colloids in trace metal transport and
801   adsorption behavior in New Jersey Pinelands streams. *Limnol. Oceanogr.* **44**,
802   1019-1034.
803 Rouxel, O., N. Dobbek, Ludden, J. and Fouquet, Y. 2003, Iron isotope fractionation
804   during oceanic crust alteration. *Chemical Geology* 202(1-2): 155-182.
805 Rouxel, O., Bekker, A., and Edwards, K., 2005. Iron Isotope Constraints on the Archean
806   and Paleoproterozoic Ocean Redox State. *Science* **307**, 1088-1091.
807 Rouxel, O., Shanks, W. C., Bach, W., and Edwards, K., 2008a. Integrated Fe and S
808   isotope study of seafloor hydrothermal vents at East Pacific Rise 9-10N. *Chem.*
809   *Geol.* **252**, 214-227.
810 Rouxel, O., Sholkovitz, E., Charette, M., and Edwards, K., 2008b. Iron Isotope
811   Fractionation in Subterranean Estuaries. *Geochem. Cosmochim. Acta* **72**, 3413-
812   3430.
813 Rouxel, O. Natural variations of Fe isotopic compositions of seawater determined by MC-
814   ICPMS. 2009. *Geophysical Research Abstracts,* 11, EGU2009-10517.
815 Rudnick, R. L. and Gao, S., 2007. Composition of the Continental Crust. *Treatise on*
816   *Geochemistry* Chapter 3.01, 1-64.
817 Schauble, E.A., 2004. Applying stable isotope fractionation theory to new systems. In:
818   Johnson, C.M., Beard, B.L., Albarede, F. (Eds.), Geochemistry of Non-traditional
819   Stable Isotopes. *Mineralogical Society of America*, Washington DC, pp. 65–111.
820 Severmann, S., Johnson, C. M., Beard, B. L., and McManus, J., 2006. The effect of early
821   diagenesis on the Fe isotope compositions of porewaters and authigenic minerals
822   in continental margin sediments. *Geochimica et Cosmochimica Acta* **70**, 2006-
823   2022.
824 Severmann, S., Lyons, T. W., Anbar, A., McManus, J., and Gordon, G., 2008. Modern
825   iron isotope perspective on the benthic iron shuttle and the redox evolution of
826   ancient oceans. *Geology* **36**, 487-490.
827 Sholkovitz, E. R., 1976. Flocculation of dissolved organic and inorganic matter during the
828   mixing of river water and seawater. *Geochimica et Cosmochimica Acta* **40**, 831-
829   845.
830 Sholkovitz, E. R., 1978. The flocculation of dissolved Fe, Mn, Al, Cu, Ni, Co and Cd
831   during estuarine mixing. *Earth and Planetary Science Letters* **41**, 77-86.
832 Sholkovitz, E. R., Boyle, E. A., and Price, N. B., 1978. The removal of dissolved humic
833   acids and iron during estuarine mixing. *Earth and Planetary Science Letters* **40**,
834   130-136.
835 Skulan, J. L., Beard, B. L., and Johnson, C. M., 2002. Kinetic and equilibrium Fe isotope
836   fractionation between aqueous Fe(III) and hematite. *Geochimica et Cosmochimica*
837   *Acta* **66**, 2995-3015.
838 Staubwasser, M., von Blanckenburg, F., and Schoenberg, R., 2006. Iron isotopes in the
839   early marine diagenetic iron cycle. *Geology*, **34**, 629–632.
840 Stookey, L. L., 1970. FerroZine– a new spectrophotometric reagent for iron. *Anal. Chem.*
841   **42**, 779-781.
842 Taylor, S. R., McLennan, S. M., and McCulloch, M. T., 1983. Geochemistry of loess,
843   continental crustal composition and crustal model ages. *Geochimica et*
844   *Cosmochimica Acta* **47**, 1897-1905.
845 Teutsch, N., vonGunten, U., Porcelli, D., Cirpka, O. A., and Halliday, A. N., 2005.
846   Adsorption as a cause for Iron Isotope fractionation in reduced groundwater.
847   *Geochim. Cosmochim. Acta* **17**, 4175-4185.

848   Thompson, A., Ruiz, J., Chadwick, O. A., Titus, M., and Chorover, J., 2007. Rayleigh
849   fractionation of iron isotopes during pedogenesis along a climate sequence of
850   Hawaiian basalt. *Chemical Geology* **238**, 72-83.
851   Upadhyay, S., 2008. Sorption model for dissolved and particulate aluminium in the
852   Conway estuary, UK. *Estuarine and Coastal Marine Science* **76**, 914-919.
853   Urey, C.H., 1947. The thermodynamic properties of isotopic substances. *J. Chem. Soc*.
854   562–581.
855   Van den Berg, C. M. G., 1995, Evidence for organic complexation of iron in seawater.
856   *Marine Chemistry* 50(1-4): 139-157.
857   Wedepohl, K. H., 1995. The composition of the continental crust. *Geochimica et*
858   *Cosmochimica Acta* **59**, 1217-1232.
859   Wells, M. L., Price, N. M., and Bruland, K. W., 1995. Iron chemistry in seawater and its
860   relationship to phytoplankton: a workshop report. *Marine Chemistry* **48**, 157-182.
861   Weyer, S. and Schwieters, J. B., 2003. High precision Fe isotope measurements with high
862   mass resolution MC-ICPMS. *International Journal of Mass Spectrometry* **226**,
863   355-368.
864   Wiederhold, J. G., Teutsch, N., Kraemer, S. M., Halliday, A. N., and Kretzschmar, R.,
865   2007. Iron isotope fractionation in oxic soils by mineral weathering and
866   podzolization. *Geochimica et Cosmochimica Acta* **71**, 5821-5833.
867   Wu, J., Boyle, E., Sunda, W., and Wen, L.-S., 2001. Soluble and colloidal iron in the
868   Oligotrophic North Atlantic and North Pacific. *Science* **293**, 847-849.
869   Yan, L., Stallard, R. F., Key, R. M., and Crerar, D. A., 1990. The chemical behavior of
870   trace metals and 226Ra during estuarine mixing in the Mullica River estuary, New
871   Jersey, U.S.A.: A comparison between field observation and equilibrium
872   calculation. *Chemical Geology* **85**, 369-381.
873   Zhuang, G., Yi, Z., and Wallace, G. T., 1995. Iron(II) in rainwater, snow, and surface
874   seawater from a coastal environment. *Marine Chemistry* **50**, 41-50.
875
876

FIGURE CAPTIONS

878

879 Figure 1: Map of the North River estuary showing sampling sites at low and high tides.

880 Sample name are also shown for each sampling site.

881

882 Figure 2: Color and concentrations of Fe, Al, Mo, Mn (μM) and Ca (mM) of the dissolved

883 fraction (<0.22 μm) versus salinity along the North River estuary. Sampling during ebb

884 (open diamonds) and flood (gray diamonds) tides are shown for comparison.

885

886 Figure 3: Concentrations of particulate Fe (>0.22 μm) and dissolved versus particulate Fe

887 ratios along the salinity profile. Sampling during ebb and flood tides are shown in open

888 and gray diamonds respectively.

889

890 Figure 4: Fraction of Fe removed (i.e. flocculation factor F) along the North River

891 estuary. Fe concentrations *vs.* salinity are shown for comparison.

892

893 Figure 5: Fe-isotope compositions of dissolved Fe (<0.22 μm) and particulate Fe (>0.22

894 μm) along the salinity gradient. Horizontal gray bar corresponds to average δ^{56}Fe values

895 for crustal rocks (Beard et al., 2001; Dauphas and Rouxel, 2006).

896

897 Figure 6: Al/Fe ratios of dissolved Fe (<0.22 μm) and particulate Fe (>0.22 μm) along the

898 salinity gradient at North River estuary.

899

900 Figure 7: Iron isotope composition of dissolved pool *versus* the fraction (F) of Fe

901 removed through flocculation process. A) a linear relationship between δ^{56}Fe and 1/(1-F)

902 is expected if truly dissolved Fe in rivers is different from riverine colloids; B) a linear

903 relationship between δ^{56}Fe and –log(1-F) is expected if colloid flocculation process

904 produce significant Fe-isotope fractionation between coagulated colloids and remaining

905 dissolved colloids.

906

907 Figure 8: (A) δ^{56}Fe *vs.* Al/Fe ratios of dissolved Fe (<0.22 μm) and particulate Fe (>0.22

908 μm) at North River estuary showing a 3-component mixing relationship between (1)

909 riverine colloids (X_{col}) (2) river borne particles (X_{RP}) and (3) lithogenic particles (X_{Litho})

910   from high salinity end-members. (B) Variations of X_{col}, X_{RP} and X_{Litho} with salinity. See

911   text for discussion.

912

913   Figure 9: Relationship between the X_{Col}/X_{RP} and the fraction (F) of Fe removed through

914   flocculation. X_{Col} and X_{RP} represent the fractions of particulate Fe from coagulated

915   colloids and river borne particles respectively. As expected, the ratio X_{Col}/X_{RP} increase

916   linearly with F along a 1:1 slope reflecting the addition of particles along the estuary due

917   to flocculation process. This relationship also suggests a minimal loss of particulate Fe

918   during estuarine mixing.

919

920

Norwell

NR 1017

NR 1018

NR 1015

NR 1022

NR 1020

NR 1013

NR 1012

NR 1010

NR 1026

NR 1024

NR 1023

NR 1021

NR 1016

NR 1014

NR 1027

NR 1009

NR 1011

NR 1008

NR 1028

NR 1007

Marshfield Hills

NR 1006

NR 1029

NR 1005

NR 1030

NR 1004

NR 1003

NR 1031

NR 1002

NR 1032

NR 1001

NR 1034

NR 1033

High Tide sampling sites

Low tide sampling sites

1000 m
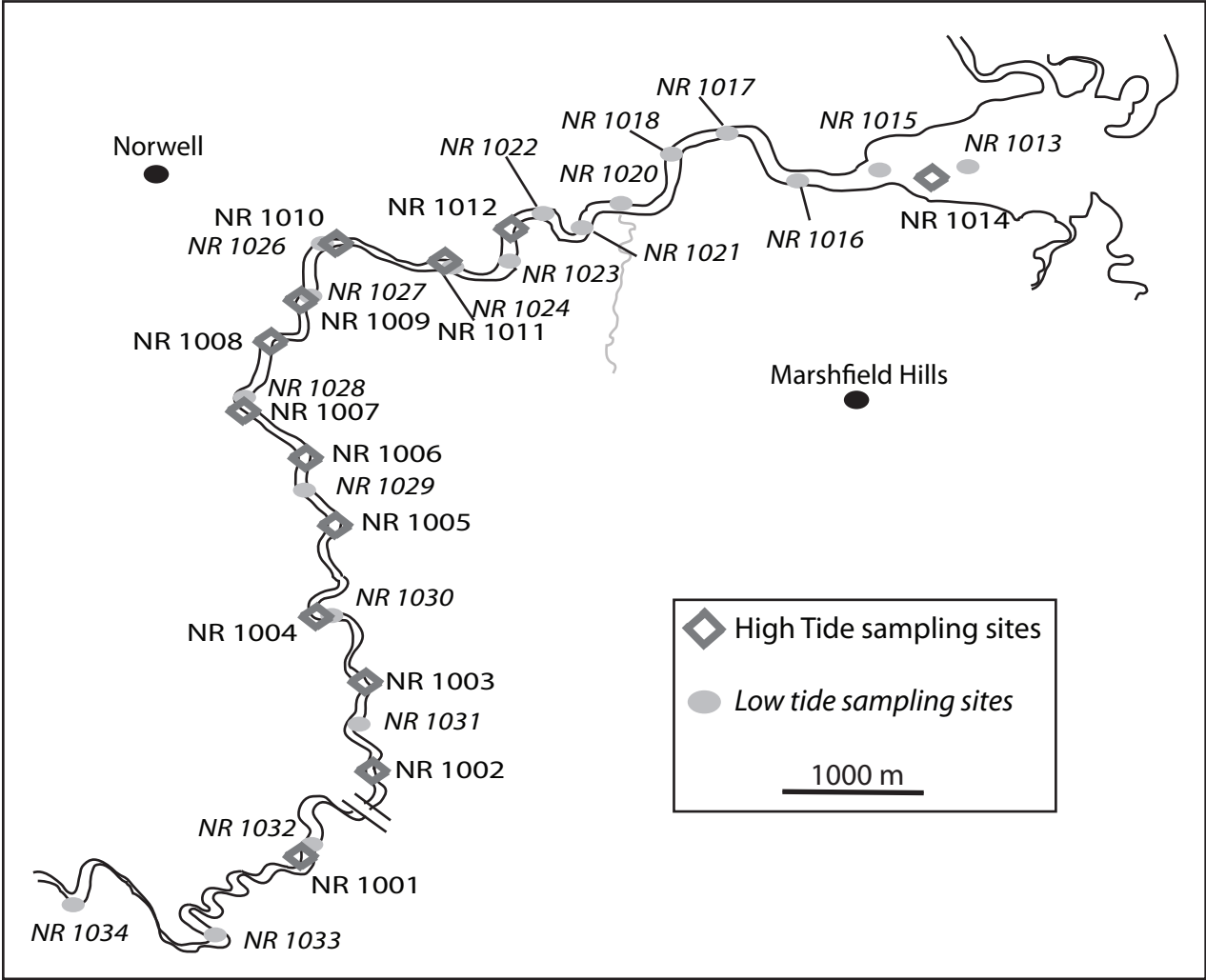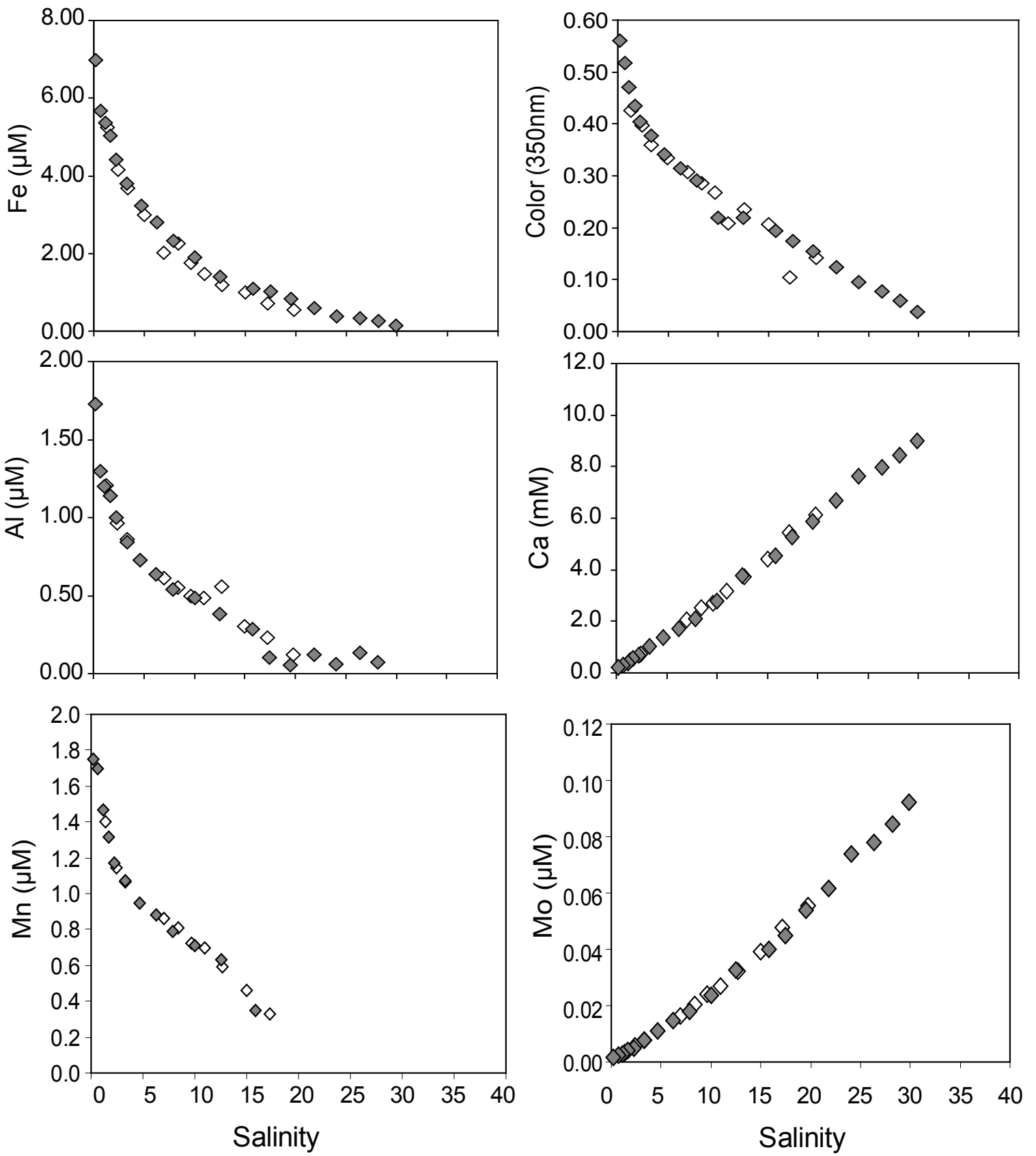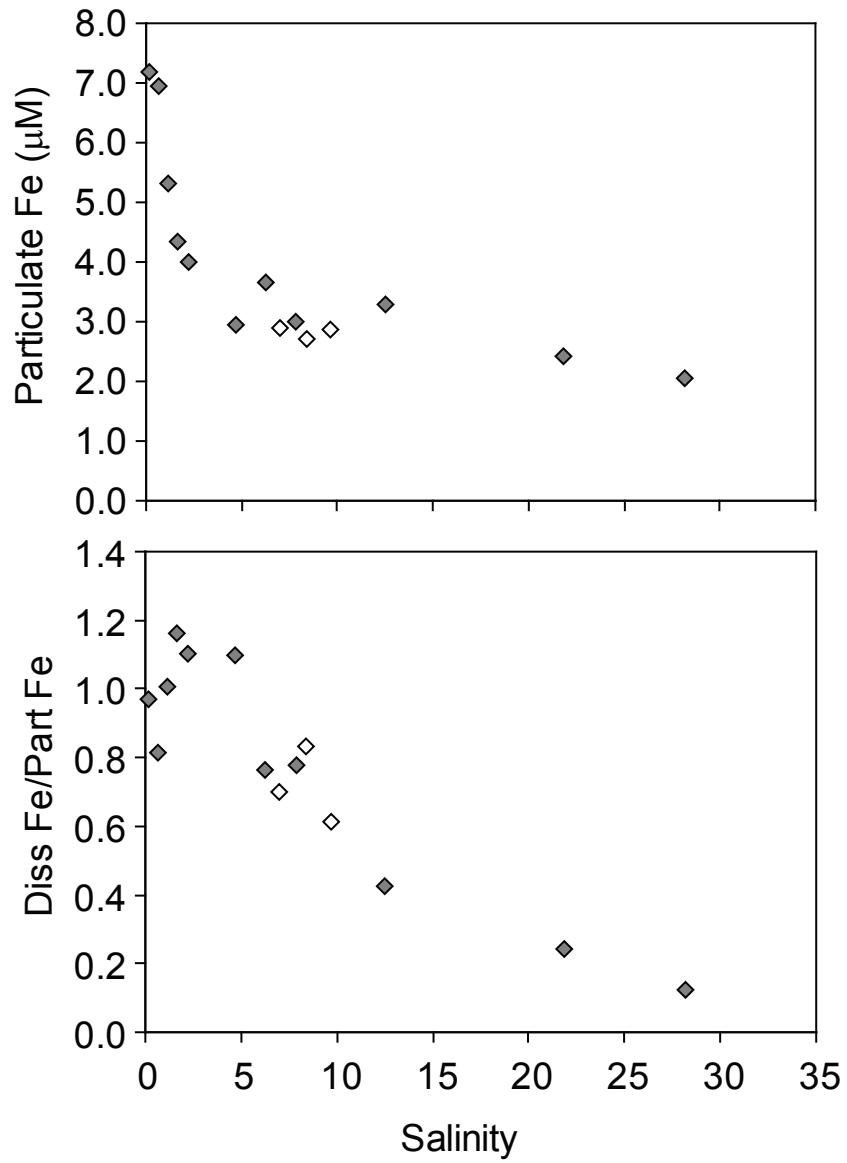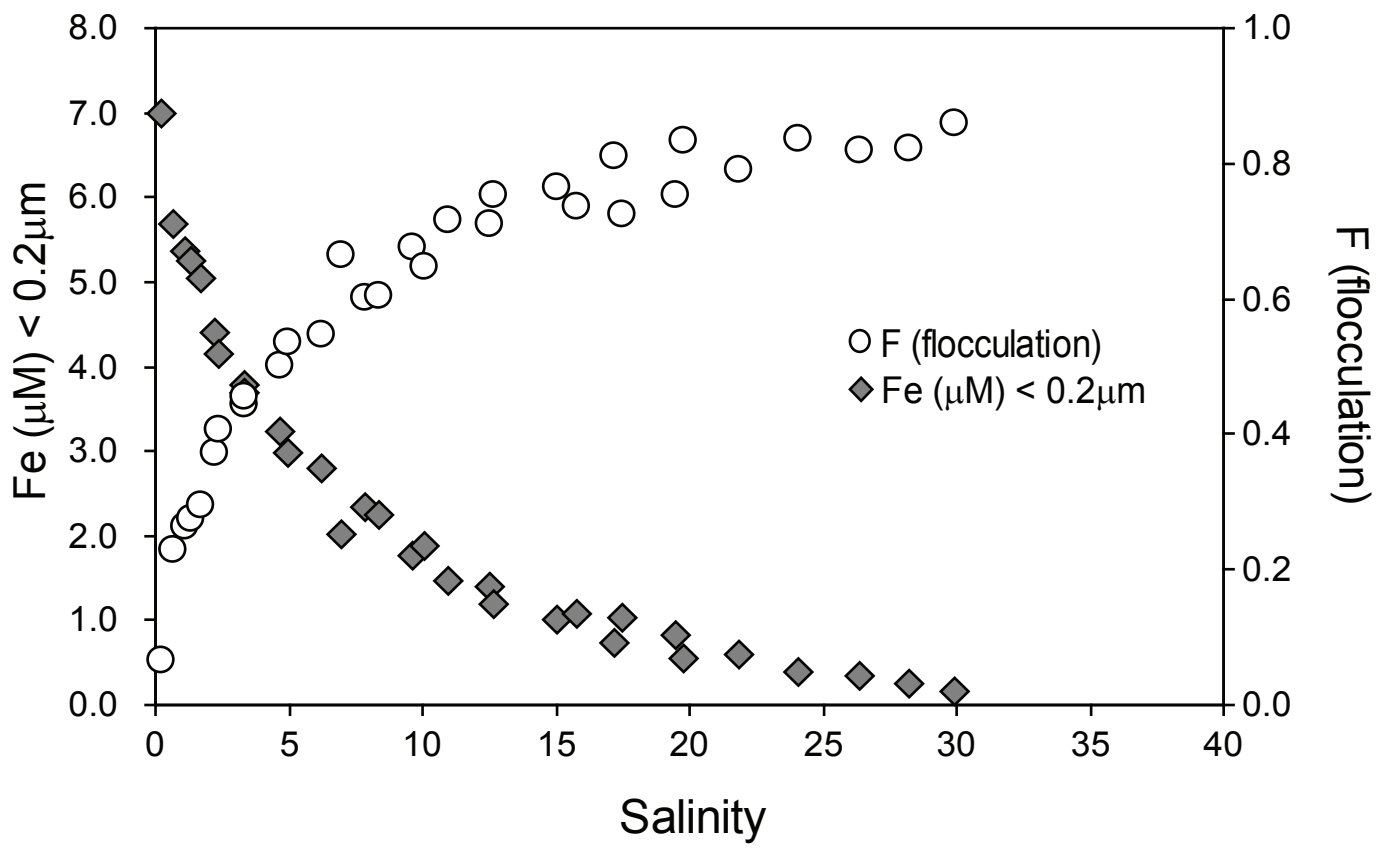
Figure 2

Figure 3

Figure 4

Figure 5

Figure 6

(A)

y = 0.0272x + 0.3744
R^2 = 0.2147

δ^{56}Fe (‰)

1/(1-F)

(B)

y = 0.1386x + 0.3906
R^2 = 0.2554

δ^{56}Fe (‰)

-log(1-F)

Figure 7

(A)

Legend:
- ◇ Dissolved Fe (<0.22 μm)
- ■ Particulate Fe (>0.22 μm)

X_{Col}

X_{Lith}

X_{RP}

y-axis: $\delta^{56}Fe$ (‰)

x-axis: Al / Fe (g/g)

(B)

Legend:
- ◇ X_{Lith}: lithogenic particules
- ■ X_{Col}: flocculated colloids
- ▲ X_{RP}: river-borne particules

y-axis: Particulate composition X

x-axis: Salinity
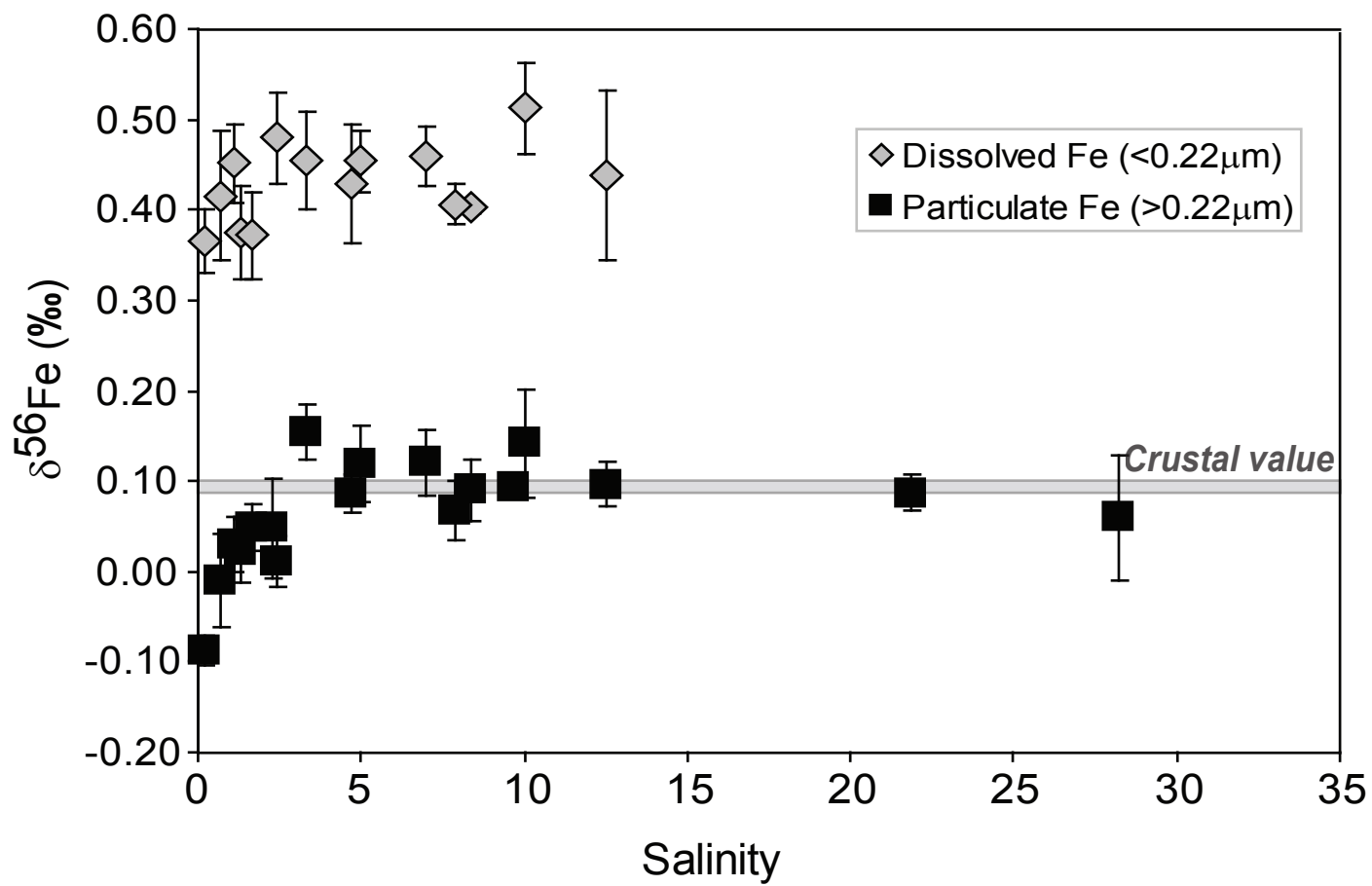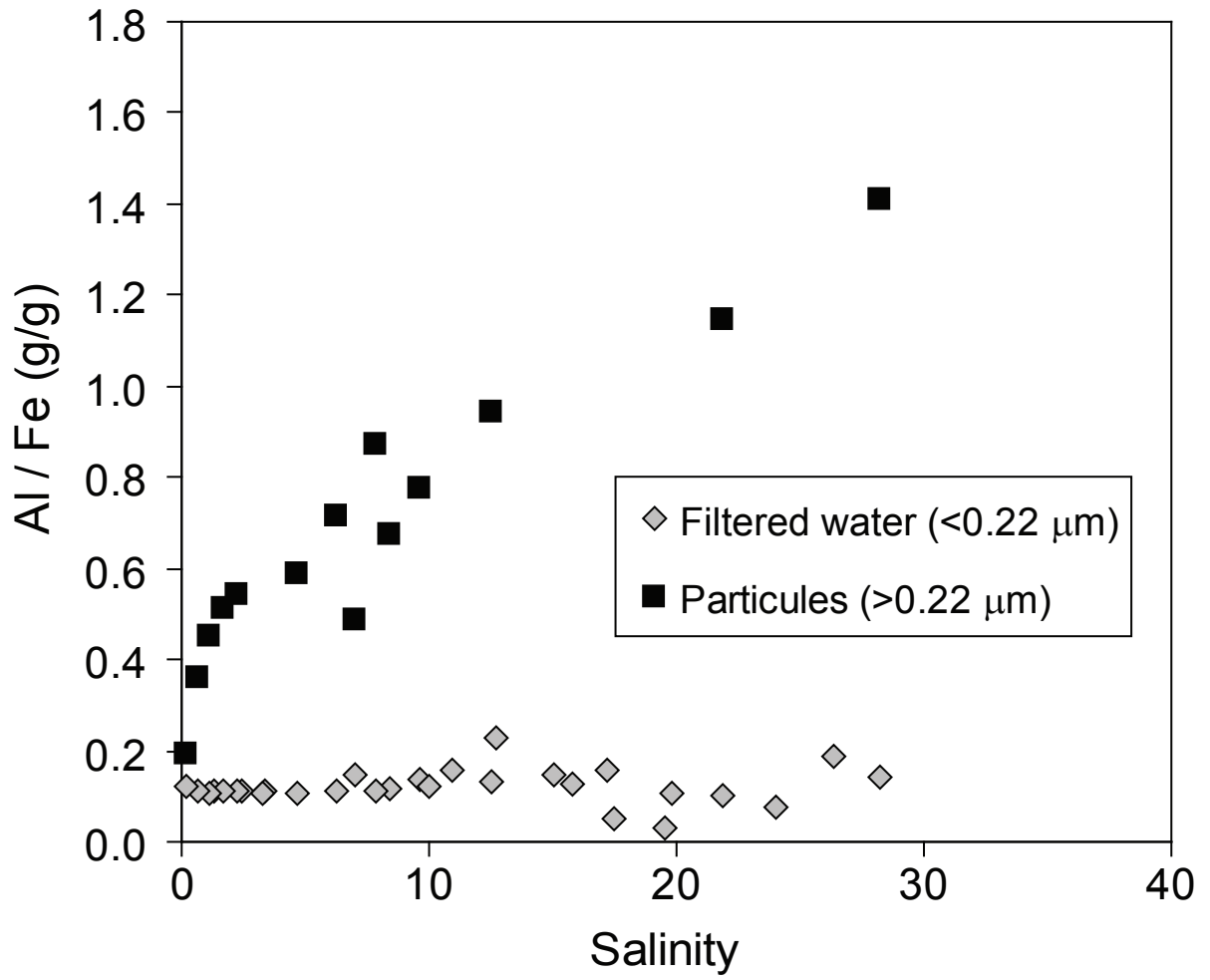
Figure 8

Figure 9

Table 1: Chemical and isotopic composition of filtered North River estuary samples

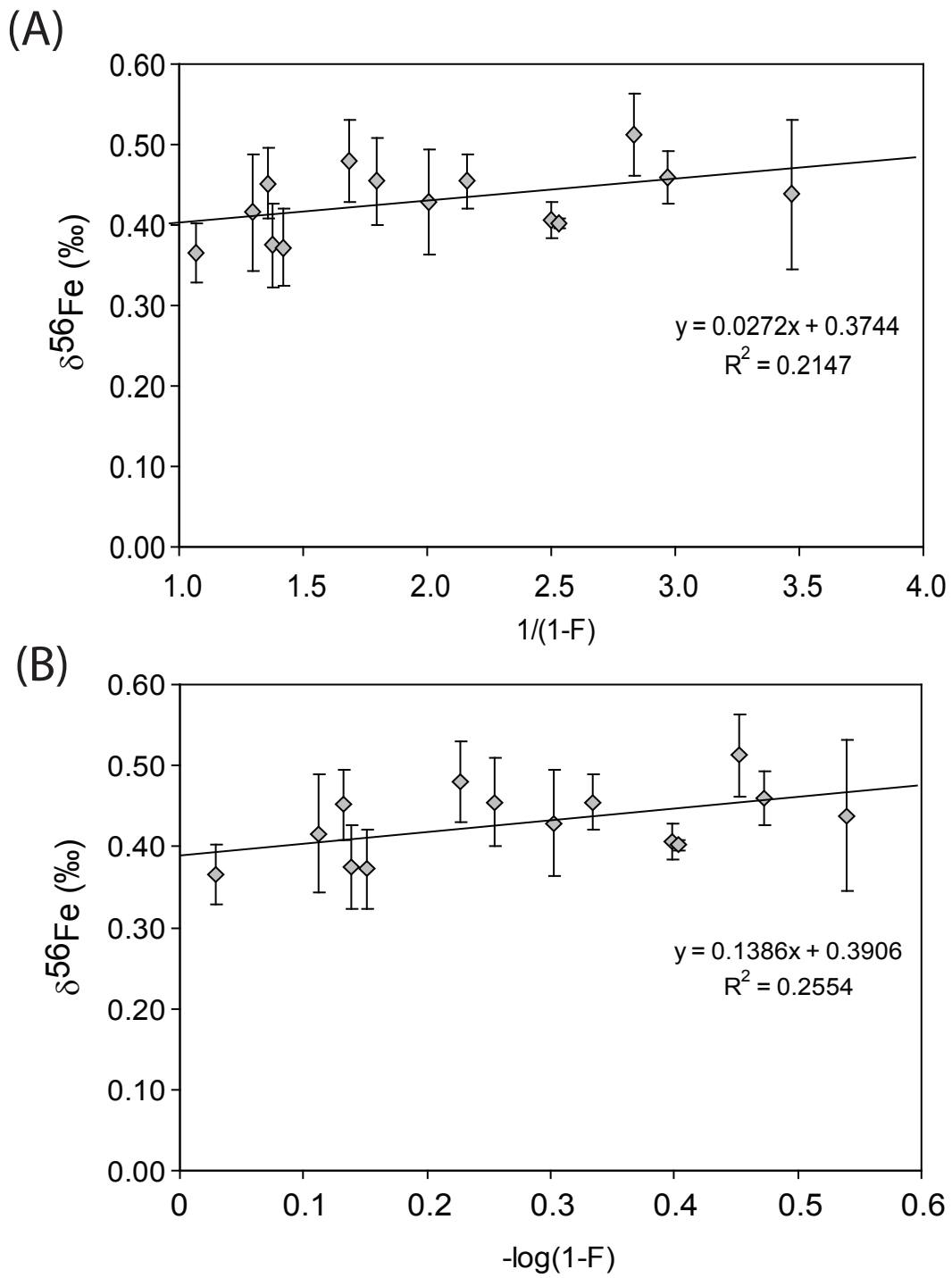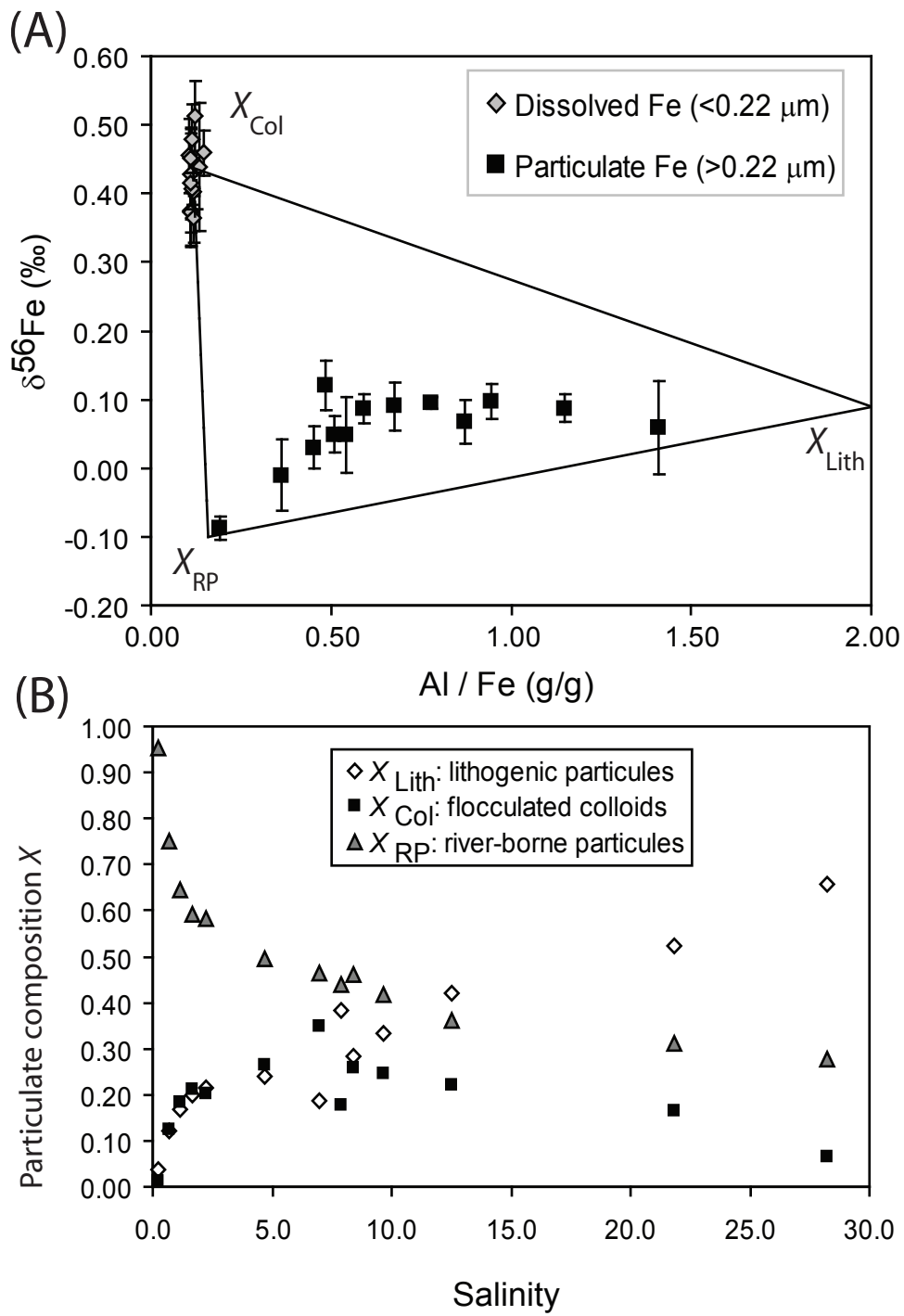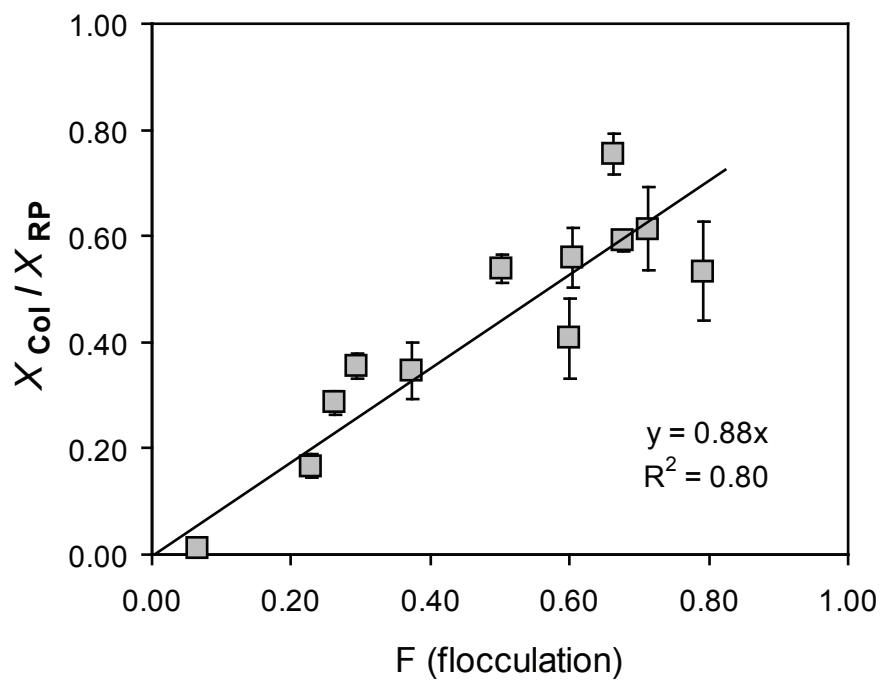| Sample Name	Salinity	color at 350 nm	Fe (μM)	Al (μM)	Ca (mM)	Mo (μM)	Mn (μM)	N#	δ^{56}Fe	1σ	δ^{57}Fe	1σ
ebb tide												
NR-1001	1.33	0.426	5.24	1.21	0.5	0.003	1.40	5	0.37	0.05	0.56	0.09
NR-1002	2.40	0.397	4.15	0.96	0.7	0.006	1.14	6	0.48	0.05	0.69	0.08
NR-1004	4.99	0.334	2.98	-	-	-	-	4	0.45	0.03	0.70	0.04
NR-1005	6.97	0.307	2.02	0.62	2.0	0.016	0.86	5	0.46	0.03	0.65	0.08
NR-1006	8.40	0.286	2.25	0.55	2.5	0.020	0.81	2	0.40	0.01	0.57	0.08
flood tide												
NR-1021	12.51	0.22	1.39	0.38	3.8	0.033	0.63	2	0.44	0.09	0.66	0.12
NR-1022	10.04	0.219	1.89	0.48	2.8	0.023	0.71	2	0.51	0.05	0.78	0.08
NR-1023	7.86	0.291	2.33	0.54	2.1	0.018	0.79	6	0.41	0.02	0.61	0.06
NR-1025	4.67	0.341	3.24	0.73	1.4	0.011	0.95	5	0.43	0.07	0.64	0.06
NR-1026	3.31	0.377	3.79	0.84	1.0	0.008	1.07	12	0.45	0.05	0.67	0.07
NR-1028	1.68	0.435	5.04	1.14	0.5	0.004	1.32	6	0.37	0.05	0.57	0.06
NR-1029	1.12	0.471	5.36	1.20	0.4	0.003	1.47	5	0.45	0.04	0.68	0.07
NR-1030	0.69	0.518	5.68	1.29	0.3	0.002	1.70	6	0.42	0.07	0.59	0.05
NR-1033	0.20	0.56	6.98	1.73	0.2	0.002	1.75	6	0.37	0.04	0.55	0.06

#: number of duplicated Fe-isotope analysis

- : not determined

Table2: Chemical and Fe-isotope composition of suspended particles in North River estuary

Sample Name	Salinity	Al (μM)	Fe (μM)	Ti (μM)	Ca (μM)	Mn (μM)	N#	δ^{56}Fe	1σ	δ^{57}Fe	1σ
NR 1001 F	1.33	-	-	-	-	-	7	0.02	0.04	0.06	0.04
NR 1002 F	2.40	-	-	-	-	-	8	0.01	0.03	0.11	0.04
NR 1004 F	4.99	-	-	-	-	-	8	0.12	0.04	0.18	0.03
NR 1005 F	6.97	2.92	2.90	0.08	2.49	0.07	8	0.12	0.04	0.23	0.06
NR 1006 F	8.4	3.79	2.71	0.10	2.80	0.06	13	0.09	0.03	0.16	0.07
NR 1007 F	9.66	4.61	2.87	0.12	3.28	0.07	5	0.09	0.01	0.17	0.02
NR 1014 F	28.2	5.98	2.05	0.17	7.88	0.04	4	0.06	0.07	0.12	0.04
NR 1017 F	21.84	5.75	2.42	0.16	6.55	0.04	7	0.09	0.02	0.11	0.06
NR 1021 F	12.51	6.42	3.29	0.19	4.56	0.07	8	0.10	0.02	0.14	0.06
NR 1022 F	10.04	-	-	-	-	-	7	0.14	0.06	0.28	0.07
NR 1023 F	7.86	5.40	3.00	0.15	3.25	0.08	10	0.07	0.03	0.11	0.06
NR 1024 F	6.25	5.43	3.66	0.17	2.93	0.09		-		-	
NR 1025 F	4.67	3.60	2.95	0.09	2.21	0.06	8	0.09	0.02	0.09	0.03
NR 1026 F	3.31	-	-	-	-	-	4	0.15	0.03	0.24	0.03
NR 1027 F	2.25	4.48	4.00	0.12	1.84	0.10	7	0.05	0.05	0.09	0.08
NR 1028 F	1.68	4.57	4.33	0.11	1.74	0.11	5	0.05	0.03	0.10	0.03
NR 1029 F	1.12	4.99	5.32	0.13	1.88	0.14	11	0.03	0.03	0.07	0.04
NR 1030 F	0.69	5.20	6.96	0.13	2.26	0.16	12	-0.01	0.05	0.00	0.08
NR 1033 F	0.2	2.85	7.19	0.07	3.04	0.15	6	-0.09	0.02	-0.11	0.04

#: number of duplicated Fe-isotope analysis

- : not determined

Table 3: Fe concentration and isotope composition of North River for different filter size

	Size fraction (μm)	[Fe] μM	N#	$\delta^{56}Fe$	1σ	$\delta^{57}Fe$	1σ
Water							
NR II E*	< 0.22*	8.65	6	0.34	0.03	0.55	0.08
NR II A	< 0.22	8.76	6	0.38	0.02	0.55	0.02
NR II B	< 0.1	8.6**	14	0.38	0.06	0.54	0.08
NR II C	< 0.05	8.2**	6	0.44	0.03	0.65	0.03
NR II D	< 0.025	8.6**	5	0.42	0.02	0.58	0.03
Particules							
NR II A F	>0.22	3.17	6	-0.22	0.01	-0.32	0.07
NR II B F	0.22 - 0.1	0.08	3	-0.12	0.04	-0.22	0.03
NR II C F	0.22 - 0.05	0.47	9	0.14	0.02	0.21	0.03
NR II D F	0.22 - 0.025	0.07	3	0.09	0.08	0.24	0.10

* filtration through 0.22um Millipak^{TM} cartridge instead of Durapore^{TM} 45mm membrane

* filtration through 0.22um Millipak^{TM} cartridge instead of Durapore^{TM} 45mm membrane

** calculated by mass balance using particulate Fe concentration

#: number of duplicated Fe-isotope analysis

Table 4: Fe-isotope composition and percent of Fe removal in North River and other east coast estuaries

Estuary	Date	River water end-member Fe (μM)	δ^{56}Fe river end-member	(1σ)	Zero-salinity intercept Fe (μM)	% removal	Reference
Connecticut	07/1973	8.5	-		2.5	71	Boyle et al., 1977
	11/1973	3.1	-		0.9	71	Boyle et al., 1977
	11/2006	1.4	**0.18**	0.03	-	-	This study
	05/2007	1.3	-		0.5	64	This study
Merrimack	07/1973	4.0	-		1.5	63	Boyle et al., 1977
	08/1973	3.5	-		1.0	71	Boyle et al., 1977
	10/1973	3.7	-		1.7	54	Boyle et al., 1977
Mullica	09/1973	23.4	-		1.0	96	Boyle et al., 1977
	06/2007	8.3	**-0.33**	0.02	-	-	This study
North River	05/2006	8.9	**0.14**	0.05	3.3	63	This study
	10/2006	7.5	**0.37**	0.04	1.4	82	This study
	11/2006	8.6	**0.34**	0.03	n.d.	n.d.	This study

- : not determined